

Notes added after first publication: ESI was updated on 28/01/2025 on NMR instrument information.

## *Electronic Supplementary Information*

### **Bright and Two-Photon Active Red Fluorescent Dyes that Selectively Move Back and Forth between Mitochondria and Nucleus upon Changing the Mitochondrial Membrane Potential**

Hitomi Seki,<sup>†</sup> Shozo Onishi,<sup>‡</sup> Naoya Asamura,<sup>‡</sup> Yasutaka Suzuki,<sup>‡</sup> Jun Kawamata,<sup>‡</sup>  
Daisuke Kaneno,<sup>§</sup> Shingo Hadano,<sup>†</sup> Shigeru Watanabe,<sup>†</sup> Yosuke Niko<sup>\*†</sup>

<sup>†</sup>Research and Education Faculty, Multidisciplinary Science Cluster, Interdisciplinary Science Unit, Kochi University, 2-5-1, Akebono-cho, Kochi-shi, Kochi, 780-8520, Japan.

<sup>‡</sup>Graduate School of Medicine, Yamaguchi University, 1677-1, Yoshida, Yamaguchi, 753-8512, Japan.

<sup>§</sup>Department of Applied Science, Graduate School of Integrated Arts and Sciences, Kochi University, 200 Otsu, Monobe, Nankoku City, Kochi 783-8502, Japan.

\* Corresponding author. E-mail: [y.niko@kochi-u.ac.jp](mailto:y.niko@kochi-u.ac.jp)

## **Table of Contents**

- 1. Instruments.**
- 2. Materials.**
- 3.  $^1\text{H}$  NMR spectra.**
- 4. Optical properties of 13PY, 16PY, and 18PY in solvents of different polarity.**
- 5. Confirmation of selective staining of 13PY, 16PY and 18PY into mitochondria in HEK293 cells.**
- 6. Time-lapse imaging of HEK293 cells stained with 13PY and 18PY after treatment with CCCP.**
- 7. Confirmation of selective staining of 13PY and 18PY into nucleus after treatment with CCCP.**
- 8. Cytotoxicity of 13PY, 16PY, and 18PY.**
- 9. Optical properties of 13PY, 16PY, 18PY, and PY-N in the presence of ctDNA.**
- 10. Time dependence of absorption and fluorescence spectra of 13PY, 16PY, 18PY, and PY in the presence of ctDNA.**
- 11. Optical properties of 13PY, 16PY, 18PY, and PY in the presence of liposomes.**
- 12. DFT calculation.**
- 13. References.**

## 1. Instruments

### NMR and high resolution mass spectrometry and elemental analysis

All the  $^1\text{H}$  NMR spectra were recorded on a 500 MHz JEOL JNM-ECA 500 instrument with tetramethylsilane (TMS) as the internal standard. High and low-resolution mass spectra (HRMS and LRMS) were ionized by electrospray ionization (ESI) or fast atomic bombardment (FAB) and obtained by Thermo Fisher Scientific LTQ Orbitrap XL mass spectrometer. Elemental analysis were carried out by using Perkin Elmer 2400II CHN Elemental Analyzer.

### Absorption, fluorescence spectroscopy, and absolute fluorescence quantum yield

The UV-Vis spectra were recorded with a JASCO V-670 UV-Vis Spectrophotometer. Fluorescence spectra were obtained using an absolute photoluminescence quantum yield measurement system (C9920-02, Hamamatsu Photonics K. K.). All photophysical measurements performed in solutions were carried out using dilute solutions (10  $\mu\text{M}$  for UV-Vis spectra and 1  $\mu\text{M}$  for fluorescence spectra and quantum yield) in 1 cm path length quartz cells at room temperature (298 K). The measurement error in  $\Phi$  values is within 3%.

### Two-photon absorption cross section

Two-photon absorption spectra were acquired *via* induced fluorescence.<sup>1</sup> The two-photon absorption cross-section was estimated by:

$$\sigma_s^{(2)} = \frac{n_s I_s C_r \Phi_r}{n_r I_r C_s \Phi_s} \sigma_r^{(2)}$$

where  $n$ ,  $I$ ,  $C$ ,  $\Phi$  and  $\sigma^{(2)}$  are the refractive index of the solvent, the luminescence intensity, the concentration, the luminescence quantum yield, and the two-photon absorption cross-section, respectively. Subscripts  $s$  and  $r$  refer to the experimental and reference samples. As a reference sample, [2-[4-[4-(dimethylamino)phenyl]-1,3-butadienyl]-1-ethylpyridinium monoperchlorate (LDS698) was used.<sup>2</sup> A femtosecond

(fs) pulsed beam from an optical parametric amplifier (OPA-800C, Spectra-Physics) pumped by a beam from a regenerative amplifier (Spitfire, Spectra-Physics) was used as the light source. The pulse duration was typically 150 to 200 fs, at a repetition rate of 1 kHz. The average incident power was 0.01–0.3 mW. The incident beam was focused by a plano-convex lens ( $f = 80$  mm), and the emitted phosphorescence was detected with a liquid-nitrogen-cooled CCD (LN/CCD-1100PB, Princeton Instruments). Samples were dissolved in DMSO at concentrations of  $5.0 \times 10^{-4}$  M.

### **Single-photon fluorescence microscopy**

Single-photon excited fluorescence images were obtained via a wide-field fluorescence microscope IX81 (OLYMPUS) equipped with digital camera DP50 (OLYMPUS). Red emission of 13PY, 16PY, and 18PY was collected by U-MW1G (excitation filter 510–560 nm, dichroic mirror 565 nm, barrier filter 590 nm). Green emission of MitoBright Green and blue emission of Hoechst 33342 was collected by U-MNIBA2 (excitation filter 470–495 nm, dichroic mirror 505 nm, barrier filter 510–550 nm) and U-MNUA2 (excitation filter 360–370 nm, dichroic mirror 400 nm, barrier filter 420–460 nm), respectively.

### **Two-photon fluorescence microscopy**

Two-photon excited fluorescence microscopy (TPFM) was carried out using a Ti:sapphire femtosecond laser (Tsunami, Spectra-Physics) as the light source. A galvano scanner (C10516, Hamamatsu Photonics) was used as the laser scanning unit. Cells were placed in a 35 mm glass-base dish. 13PY, 16PY, and 18PY was excited by a 890 nm femtosecond laser through an oil immersion objective (Plan 60X, OLYMPUS, Tokyo, Japan). The sample was put on a power stage and scanned along the optical axis. A photomultiplier tube (R928, Hamamatsu Photonics) was used for signal detection.

### **Computational methodology**

The equilibrium structures of the compounds investigated in this work were fully optimized by using the M062X method with 6-31+G\*\* basis set. Counter anions were removed from molecular structures to avoid the burden during calculation. The Analytical frequencies were obtained to ensure that a local energy minimum has been located. Then, the singlet-spin excited states for the minima have been calculated by time-dependent density functional theory (TD-DFT).<sup>3</sup>

## 2. Materials

### Chemicals

Unless otherwise noted, all reagents and chemicals were used without further purification.

*N*-Bromosuccinimide, diisobutylaluminum hydride, triisopropylsilyl chloride, imidazole, Dess-Martin periodinate, and 4-methylpyridine were obtained from TCI (Tokyo, Japan). 1-Pyrenecarbaldehyde, *n*-butyllithium, iodomethane, Rhodamine 123, iodoethane, and TE buffer (10mM Tris-HCl, 1mM EDTA, pH 8.0) were purchased from Wako Pure Chem. (Tokyo, Japan). Tetrabutylammonium fluoride was obtained from Sigma-Aldrich (Tokyo, Japan). Piperidine, spectrograde DMSO, methanol, ethanol, DMF, 1,4-Dimethylpyridin-1-ium iodide were prepared according to previous report.<sup>4</sup> MitoBright Green, Hoechst 33342 and WST-8 were purchased from DOJINDO (Kumamoto, Japan). PY-N was prepared according to a previous literature.<sup>5</sup>

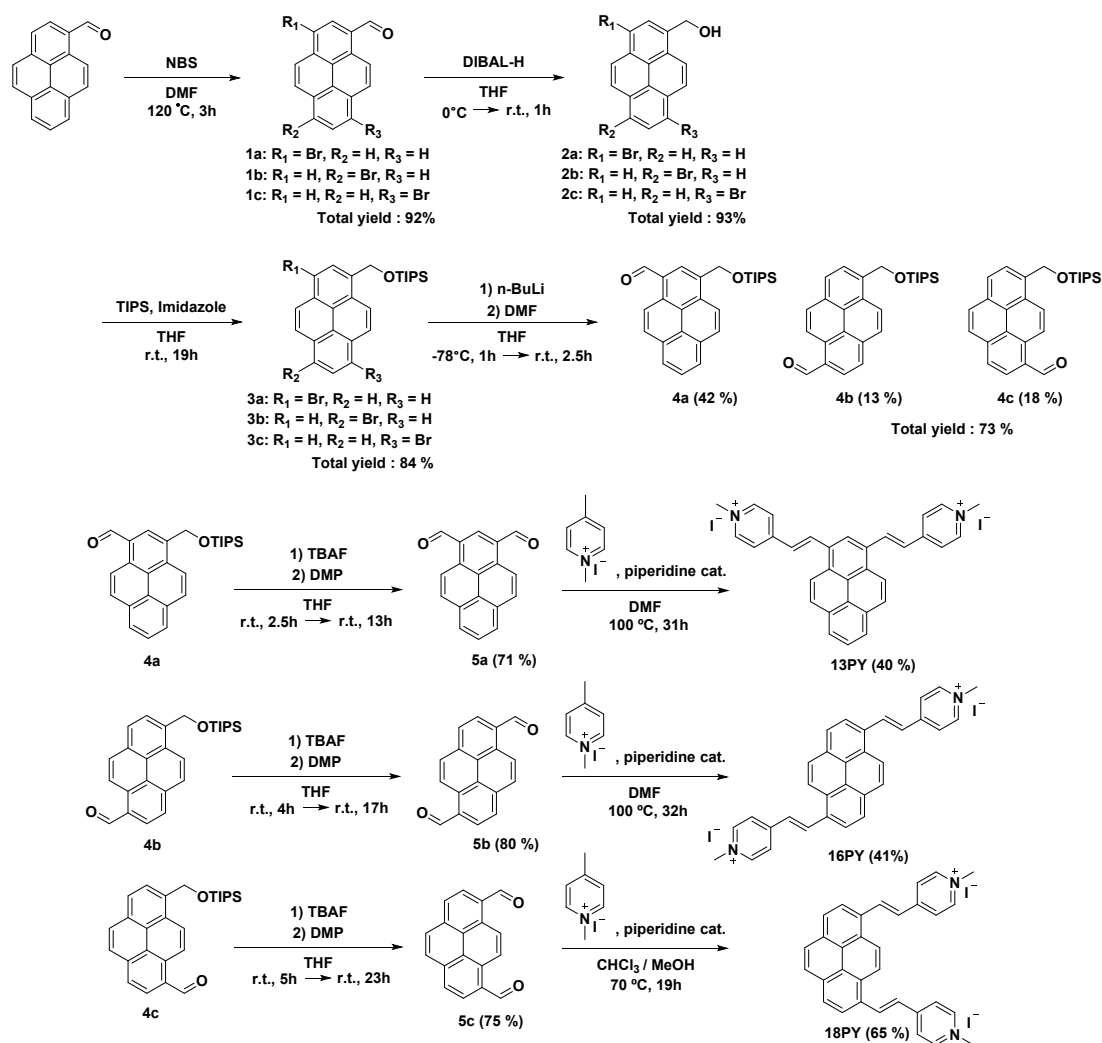
Deoxyribonucleic Acid Sodium Salt from Calf Thymus was purchased from Nacalai Tasque (Kyoto, Japan). All the experiments using CT-DNA were carried out in TE buffer. 2 mg/mL of DNA solution was prepared according to the literature methods.<sup>5</sup>

1,2-Dioleoyl-sn-glycero-3-phosphocholine (DOPC) was obtained from Sigma-Aldrich (Tokyo, Japan), and the liposomes (large uni-lamellar vesicles (LUVs)) consist of DOPC were prepared according to the literature methods.<sup>6</sup>

### Cell lines, culture conditions and treatment

HEK293 cells were grown in Dulbecco's modified Eagle medium (DMEM, Sigma-Aldrich Japan), supplemented with 10% fetal bovine serum (FBS, Sigma-Aldrich Japan) at 37 °C in a humidified atmosphere containing 5% CO<sub>2</sub>. HEK293 cell were treated with medium containing 0.5 μM of 13PY, 16PY and 18PY for 16 hours. HEK293 cells were further treated with a 0.5 μM of MitoBright Green (Invitrogen) for 30 minutes. For imaging, HEK293 cells were washed several times with phenol-red-free medium Opti-MEM (Invitrogen) supplemented with 10% (v/v) FBS. For controlling the MMP, carbonyl cyanide *m*-chlorophenyl hydrazine (CCCP), a well-known uncoupler was employed. HEK293 cell stained with 13PY, 16PY and 18PY were further treated with 30 μM of CCCP for 10 minutes.

## Synthetic details



**Scheme S1.** Synthesis of **13PY**, **16PY**, and **18PY**.

### Synthesis of 3-Bromopyrene-1-carbaldehyde (**1a**), 6-Bromopyrene-1-carbaldehyde (**1b**), 8-Bromopyrene-1-carbaldehyde (**1c**)

*N*-bromosuccinimide (8.5 g, 47.8 mmol) was added to a solution of 1-formylpyrene (10 g, 43.4 mmol) in 150 mL of DMF. The mixture was heated to reflux at 120 °C for 3 h before water were added. The resulting precipitate was collected by filtration, washed with methanol, and dried in vacuo to afford a mixture of **1a-c** (12.3 g, 92%). These crude products were used in next step without further purification. The mixture of **1a-1c** were characterized by <sup>1</sup>H NMR, measuring the integration ratio between hydrogen resonances derived from the formyl groups at 10.6-10.8 ppm and aromatic at 8.0-10.5 ppm.

**Synthesis of 3-Bromo-1-hydroxymethylpyrene (2a), 6-Bromo-1-hydroxymethylpyrene (2b), 8-Bromo-1-hydroxymethylpyrene (2c)**

A 1.0 M solution of diisobutylaluminum hydride in THF (40.4 mL, 40.4 mmol) was added dropwise to a mixture of **1a-c** (6.23 g, 20.2 mmol) in anhydrous THF (100 mL) at 0 °C under argon atmosphere. The reaction mixture was stirred at room temperature for 1 h and the progress of the reaction was monitored by TLC. The solvent was evaporated in vacuo to be minimum volume and then water was added. The resulting precipitate was collected by filtration, re-dissolved in THF, dried over MgSO<sub>4</sub>, and filtered. All volatiles were removed in vacuo to afford **2a-2c** as yellow solids (5.85 g, 93 %). The mixture of **2a-c** were characterized by <sup>1</sup>H NMR, measuring the integration ratio between hydrogen resonances derived from the hydroxymethyl groups at 5.2-5.7 ppm and aromatic at 8.0-8.6 ppm, as well as from the disappearance of the peak associated with the formyl groups.

**Synthesis of 3-Bromo-1-triisopropylsilyloxymethylpyrene (3a), 6-Bromo-1-triisopropylsilyloxymethylpyrene (3b), 8-Bromo-1-triisopropylsilyloxymethylpyrene (3c)**

Triisopropylsilyl chloride (7.51 mL, 35.4 mmol) was added to a solution of **2a-c** (5.52 g, 17.7 mmol) and imidazole (4.82 g, 70.8 mmol) in anhydrous DMF (50 mL) under an argon atmosphere. The reaction mixture was stirred at room temperature for 19 h and the progress of the reaction was monitored by TLC. After water was added, the mixture was extracted with three times with ethyl acetate. The combined organic layers were washed with water and brine, dried over MgSO<sub>4</sub>, and filtered. The solvents were evaporated in vacuo, and the residue was purified by column chromatography on silica gel (hexane:dichloromethane = 9:1) to afford **3a-c** as yellow solids (6.97 g, 84 %). The mixture of **3a-3c** were characterized by <sup>1</sup>H NMR, measuring the integration ratio between hydrogen resonances derived from the triisopropylsilyl group at 1.1-1.3 ppm, the benzyl position at 5.5-5.6 ppm, and aromatic at 7.9-8.5 ppm, as well as from the disappearance of the peak associated with the hydroxyl methyl group.

**Synthesis of 3-Formyl-1-triisopropylsilyloxymethylpyrene (4a), 6-Formyl-1-triisopropylsilyloxymethylpyrene (4b), 8-Formyl-1-triisopropylsilyloxymethylpyrene (4c)**

A 1.6 M solution of *n*-butyllithium in hexane (27.7 mL, 72.0 mmol) was added dropwise to a mixture of **3a-c** (6.51 g, 13.9 mmol) in anhydrous THF (50 mL) at -78

°C under an argon atmosphere. After the mixture was stirred for 1 h at this temperature, anhydrous DMF (2.14 mL, 27.8 mmol) was added dropwise. The mixture was warmed to room temperature and stirred for 2.5 h. After adding water, the mixture was extracted with three times with ethyl acetate. The combined organic layers were washed with water and brine, dried over MgSO<sub>4</sub>, and filtered. The solvents were evaporated in vacuo, and the residue was purified by column chromatography on silica gel (chloroform:hexane = 7:3) to afford **4a–c** as yellow solids. The yields of objective compounds were 42% for **4a** (2.46 g), 13% for **4b** (750 mg), and 18% for **4c** (1.02 g). The *R<sub>f</sub>* values of **4a–c** in the column chromatography on silica gel (chloroform:hexane=7:3) decrease in the order **4a** > **4c** > **4b**.

**4a:** <sup>1</sup>H NMR (500 MHz, CDCl<sub>3</sub>, TMS) δ 1.16 (d, *J* = 7.37, 18H), 1.25-1.34 (m, 3H), 5.58 (s, 2H), 8.08 (t, *J* = 15.34, 1H), 8.28 (m, 5H), 8.67 (s, 1H), 9.46 (d, *J* = 9.26, 1H), 10.77 (s, 1H); LRMS (FAB) Calcd for C<sub>27</sub>H<sub>32</sub>O<sub>2</sub>Si: 416.22, Found: 417 ([M + H]<sup>+</sup>).

**4b:** <sup>1</sup>H NMR (500 MHz, CDCl<sub>3</sub>, TMS) δ 1.15 (d, *J* = 7.08, 18H), 1.25-1.32 (m, 3H), 5.60 (s, 2H), 8.14 (d, *J* = 9.19, 1H), 8.26-8.32 (m, 4H), 8.43-8.45 (m, 2H), 9.38 (d, *J* = 9.19, 1H), 10.79 (s, 1H); LRMS (FAB) Calcd for C<sub>27</sub>H<sub>32</sub>O<sub>2</sub>Si: 416.22, Found: 417 ([M + H]<sup>+</sup>).

**4c:** <sup>1</sup>H NMR (500 MHz, CDCl<sub>3</sub>, TMS) δ 1.15 (d, *J* = 7.08, 18H), 1.25-1.32 (m, 3H), 5.60 (s, 2H), 8.14 (d, *J* = 9.19, 1H), 8.26-8.32 (m, 4H), 8.43-8.45 (m, 2H), 9.38 (d, *J* = 9.19, 1H), 10.79 (s, 1H); LRMS (FAB) Calcd for C<sub>27</sub>H<sub>32</sub>O<sub>2</sub>Si: 416.22, Found: 417 ([M + H]<sup>+</sup>).

### Synthesis of 1,3-pyrenedicarbaldehyde (**5a**)

A 1 M solution of tetrabutylammonium fluoride in hexane (1.08 mL, 1.08 mmol) was added dropwise to **4a** (150 mg, 0.361 mmol) in anhydrous THF (1 mL) under an argon atmosphere. After the reaction mixture was stirred for 2.5 h at room temperature, Dess-Martin periodinate (458.1 mg, 1.08 mmol) was directly added to the mixture. After stirring for 13 h the mixture was treated with water, and then the resulting precipitate was collected by filtration, and the mixture was purified by short-plug column chromatography on silica gel (chloroform) to afford objective compounds as a yellow solid (66.1 mg, 71 %). <sup>1</sup>H NMR spectrum of **5a** agreed well with previous report.<sup>7</sup> <sup>1</sup>H NMR (500 MHz, CDCl<sub>3</sub>, TMS) δ 8.19 (t, *J* = 15.31, 1H), 8.43-8.48 (m, 4H), 8.84 (s, 1H), 9.50 (d, *J* = 9.19, 2H), 10.77 (s, 2H).

### Synthesis of 1,6-pyrenedicarbaldehyde (**5b**)

A 1 M solution of tetrabutylammonium fluoride in hexane (1.08 mL, 1.08 mmol) was added dropwise to **4b** (150.3 mg, 0.361 mmol) in anhydrous THF (1.8 mL) under an

argon atmosphere. After the reaction mixture was stirred for 4 h at room temperature, Dess-Martin periodinate (458.1 mg, 1.08 mmol) was directly added to the mixture. After stirring for 13 h the mixture was treated with water, and then the resulting precipitate was collected by filtration, and the mixture was purified by column chromatography on silica gel (chloroform) to afford objective compounds as a yellow solid (74.9 mg, 80 %). <sup>1</sup>H NMR spectrum of **5b** agreed well with previous report.<sup>7</sup> <sup>1</sup>H NMR (500 MHz, CDCl<sub>3</sub>, TMS) δ 8.36 (d, *J* = 9.26, 2H), 8.38 (d, *J* = 7.87, 2H), 8.55 (d, *J* = 7.87, 2H), 9.60 (d, *J* = 9.26, 2H), 10.81 (s, 2H).

#### Synthesis of 1,8-pyrenedicarbaldehyde (**5c**)

A 1 M solution of tetrabutylammonium fluoride in hexane (2.16 mL, 2.16 mmol) was added dropwise to **4c** (300 mg, 0.72 mmol) in anhydrous THF (1.4 mL) under an argon atmosphere. After the reaction mixture was stirred for 5 h at room temperature, Dess-Martin periodinate (458.1 mg, 1.08 mmol) was directly added to the mixture. After stirring for 13 h the mixture was treated with water, and then the resulting precipitate was collected by filtration, and the mixture was purified by column chromatography on silica gel (chloroform) to afford objective compounds as a yellow solid (139.0 mg, 75 %). <sup>1</sup>H NMR spectrum of **5c** agreed well with previous report.<sup>7</sup> <sup>1</sup>H NMR (500 MHz, CDCl<sub>3</sub>, TMS) δ 8.26 (s, 2H), 8.40 (d, *J* = 7.87, 2H), 8.55 (d, *J* = 7.87, 2H), 9.62 (s, 2H), 10.86 (s, 2H).

#### Synthesis of 4,4'-((1*E*,1'*E*)-pyrene-1,3-diylbis(ethene-2,1-diyl))bis(1-methylpyridin-1-ium) iodide (**13PY**)

To a solution of **5a** (66.1 mg, 0.260 mmol) and 1,4-dimethylpyridin-1-ium iodide (305.6 mg, 1.3 mmol) in 5 mL of DMF was added a catalytic amount of piperidine (15 drops), then the mixture was heated to reflux at 100 °C for 31 h. The solvents were removed in vacuo and the crude residue was washed with hot CHCl<sub>3</sub> and MeOH to give objective compounds as an orange solid (83.4 mg, 40 %). <sup>1</sup>H NMR (500 MHz, DMSO) δ 4.29 (s, 6H), 8.02 (d, *J* = 15.52, 2H), 8.17 (t, *J* = 15.52, 1H), 8.44 (d, *J* = 6.47, 2H), 8.45 (d, *J* = 5.04, 2H), 8.54 (d, *J* = 6.47, 4H), 8.94 (m, 6H), 9.09 (s, 1H), 9.11 (d, *J* = 5.04, 2H); HRMS (ESI) Calcd for C<sub>32</sub>H<sub>26</sub>N<sub>2</sub><sup>2+</sup>: 219.10425, Found: 219.10397 ([M]<sup>2+</sup>); Anal. Calcd for C<sub>32</sub>H<sub>26</sub>N<sub>2</sub>I<sub>2</sub>: C, 55.51; H, 3.79; N, 4.05. Found: C, 55.22; H, 3.81; N, 4.18.

#### Synthesis of 4,4'-((1*E*,1'*E*)-pyrene-1,6-diylbis(ethene-2,1-diyl))bis(1-methylpyridin-1-ium) iodide (**16PY**)

To a solution of **5b** (74.9 mg, 0.290 mmol) and 1,4- dimethylpyridin-1-ium iodide (340.9 mg, 1.549 mmol) in 5 mL of DMF was added a catalytic amount of piperidine (15 drops), then the mixture was heated to reflux at 100 °C for 32 h. The solvents were removed in vacuo and the crude residue was washed with hot DMF to give objective compounds as a red solid (85.4 mg, 41 %). <sup>1</sup>H NMR (500 MHz, DMSO) δ 4.28 (s, 6H), 7.86 (d, *J* = 15.81, 2H), 8.40 (d, *J* = 9.26, 2H), 8.48 (d, *J* = 8.37, 2H), 8.49 (d, *J* = 6.72, 4H), 8.69 (d, *J* = 8.37, 2H), 8.91 (d, *J* = 6.72, 4H), 9.03 (d, *J* = 9.26, 2H), 9.10 (d, *J* = 15.81, 2H); HRMS (ESI) Calcd for C<sub>32</sub>H<sub>26</sub>N<sub>2</sub><sup>2+</sup>: 219.10425, Found: 219.10394 ([M]<sup>2+</sup>); Anal. Calcd for C<sub>32</sub>H<sub>26</sub>N<sub>2</sub>I<sub>2</sub>: C, 55.51; H, 3.79; N, 4.05. Found: C, 55.16; H, 3.75; N, 4.21.

#### **Synthesis of 4,4'-((1*E*,1'*E*)-pyrene-1,8-diylbis(ethene-2,1-diyl))bis(1-methylpyridin-1-ium) iodide (18PY)**

To a solution of **5c** (139.0 mg, 0.538 mmol) and 1,4- dimethylpyridin-1-ium iodide (305.6 mg, 1.3 mmol) in 40 mL of chloroform and 30 mL of MeOH was added a catalytic amount of piperidine (15 drops), then the mixture was heated to reflux at 70 °C for 19 h. The solvents were removed in vacuo and the crude residue was washed with hot CHCl<sub>3</sub> and MeOH to give objective compounds as a red-brown solid (242.1 mg, 65 %). <sup>1</sup>H NMR (500 MHz, DMSO) δ 4.28 (s, 6H), 7.88 (d, *J* = 15.98, 2H), 8.32 (s, 2H), 8.45 (d, *J* = 8.33, 2H), 8.51 (d, *J* = 6.72, 4H), 8.68 (d, *J* = 8.33, 2H), 8.92 (d, *J* = 6.72, 4H), 9.04 (s, 2H), 9.13 (d, *J* = 15.98, 2H); HRMS (ESI) Calcd for C<sub>32</sub>H<sub>26</sub>N<sub>2</sub><sup>2+</sup>: 219.10425, Found: 219.10396 ([M]<sup>2+</sup>); Anal. Calcd for C<sub>32</sub>H<sub>26</sub>N<sub>2</sub>I<sub>2</sub>: C, 55.51; H, 3.79; N, 4.05. Found\*: C, 52.37; H, 3.77; N, 3.70.

\*The value would be corresponding to that of 18PY dihydrate (C, 52.77; H, 4.15; N, 3.85).

### 3. $^1\text{H}$ NMR spectra.

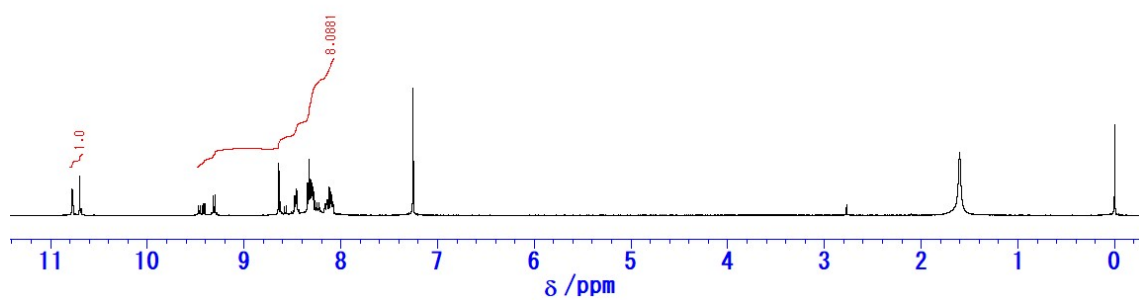


**Fig. S1**  $^1\text{H}$  NMR spectra of **1a-1c** ( $\text{CDCl}_3$ ).

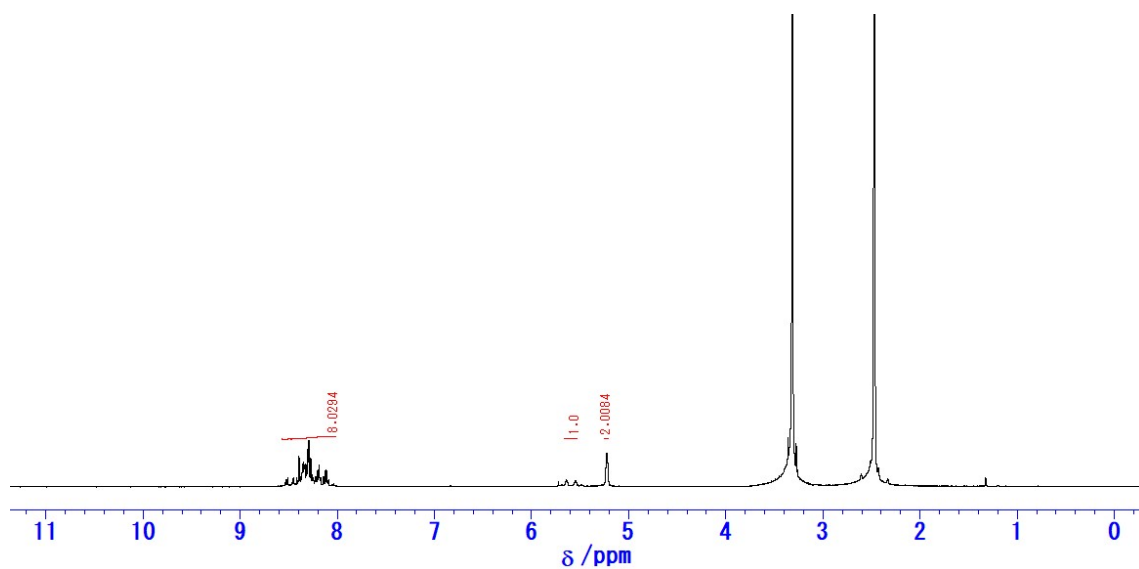


**Fig. S2**  $^1\text{H}$  NMR spectra of **2a-2c** (DMSO).

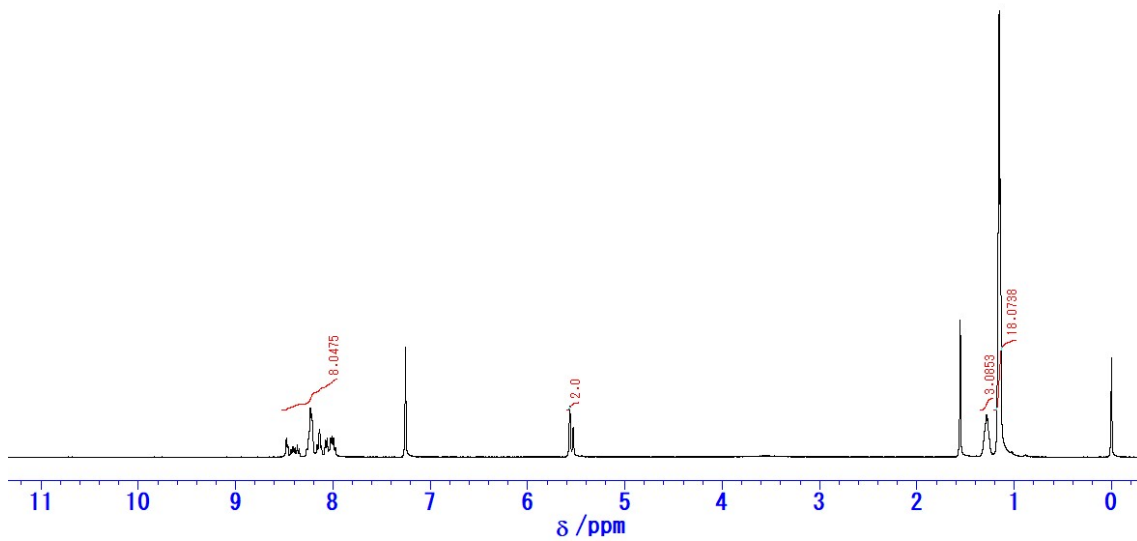


Fig. S3  $^1\text{H}$  NMR spectra of **3a-3c** ( $\text{CDCl}_3$ ).

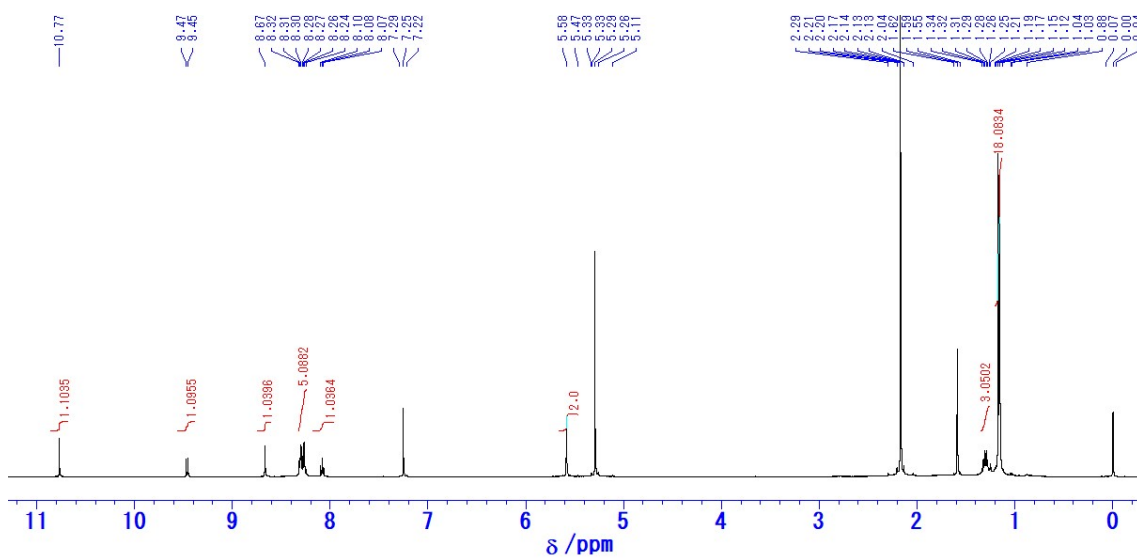


Fig. S4  $^1\text{H}$  NMR spectra of **4a** ( $\text{CDCl}_3$ ).

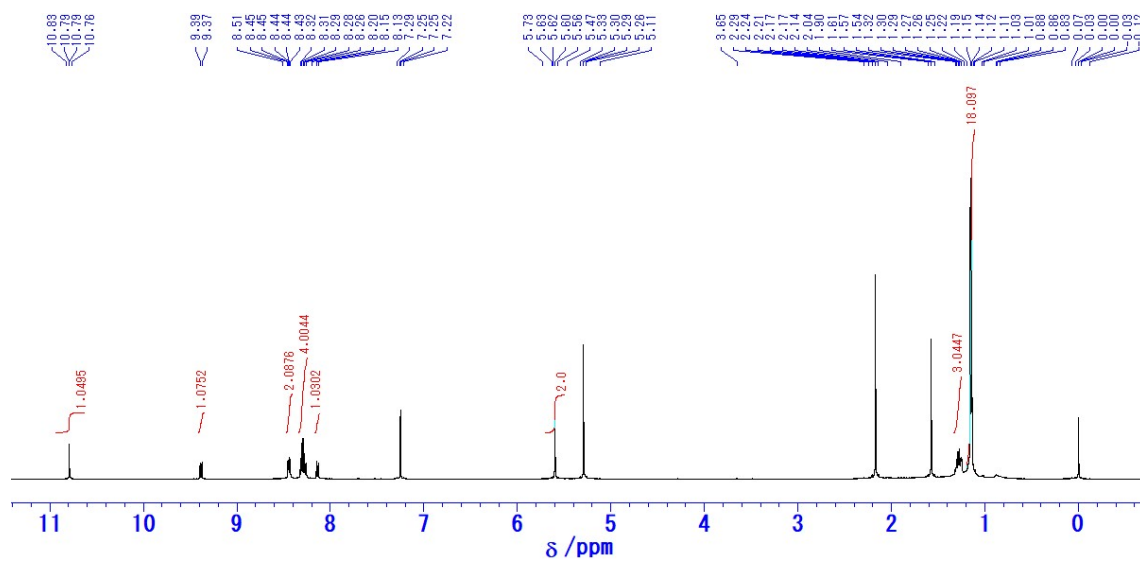


Fig. S5  $^1\text{H}$  NMR spectra of **4b** ( $\text{CDCl}_3$ ).

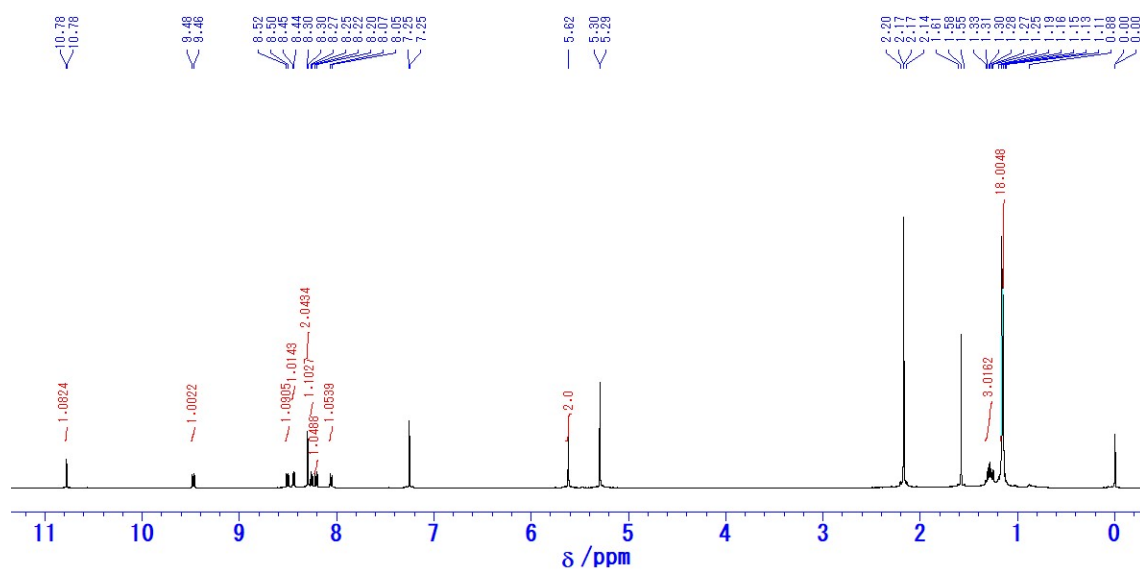
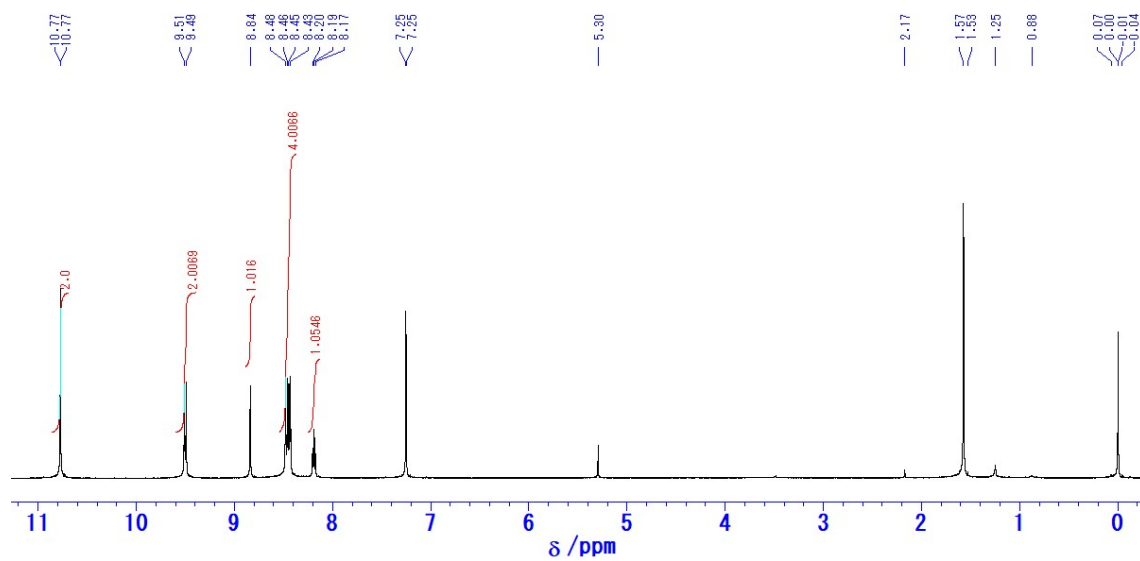
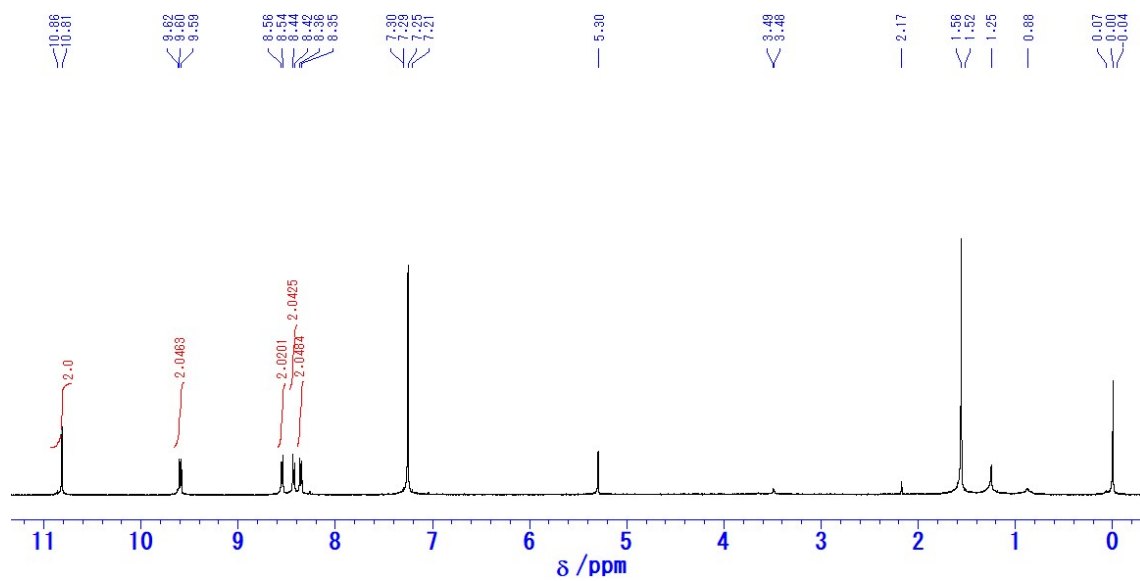


Fig. S6  $^1\text{H}$  NMR spectra of **4c** ( $\text{CDCl}_3$ ).



**Fig. S7**  $^1\text{H}$  NMR spectra of **5a** ( $\text{CDCl}_3$ ).



**Fig. S8**  $^1\text{H}$  NMR spectra of **5b** ( $\text{CDCl}_3$ ).

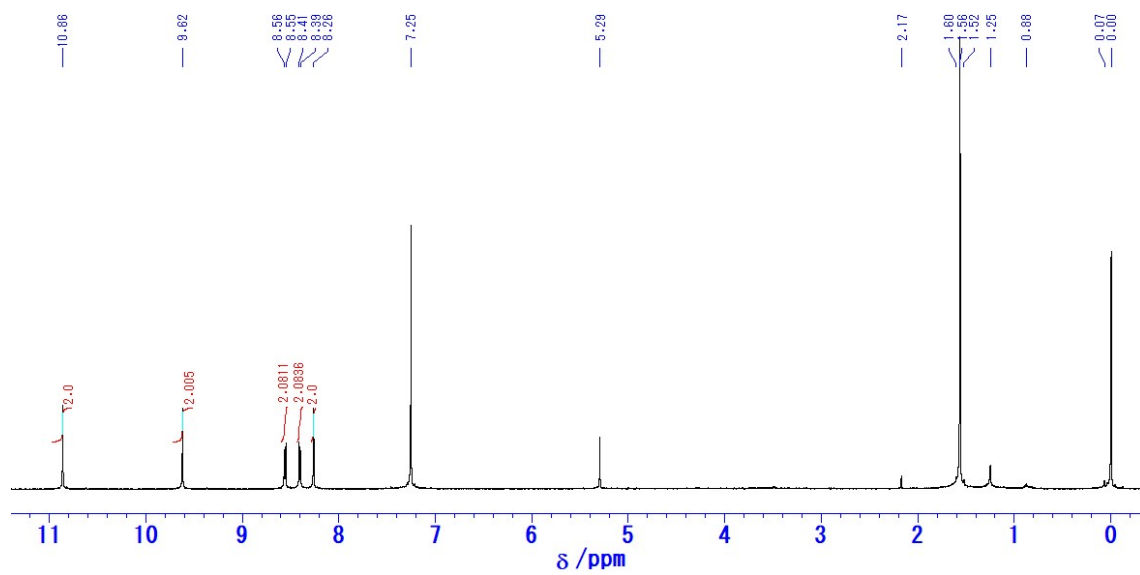
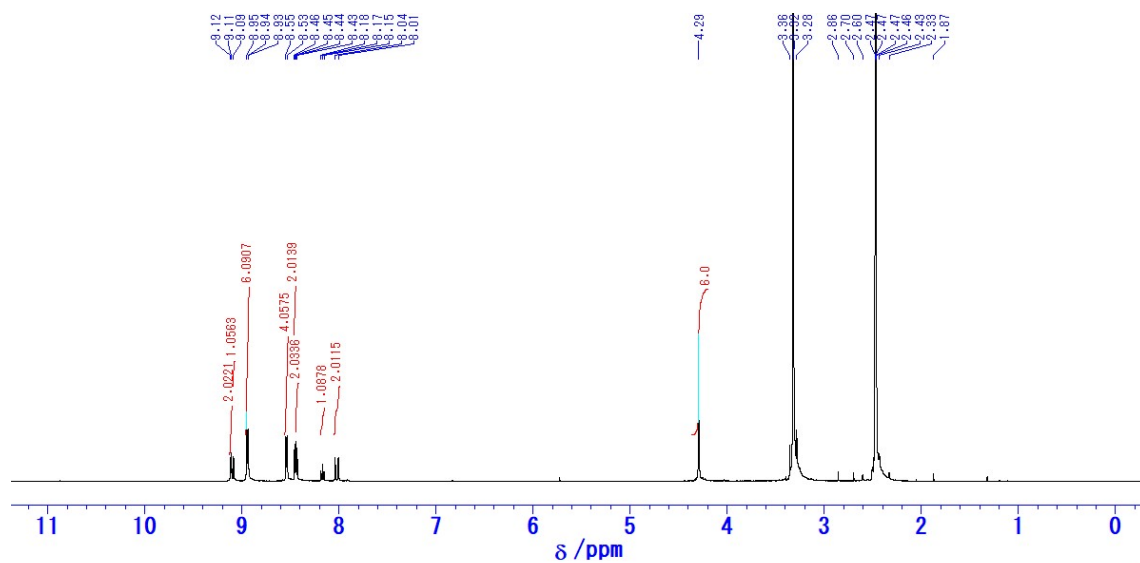


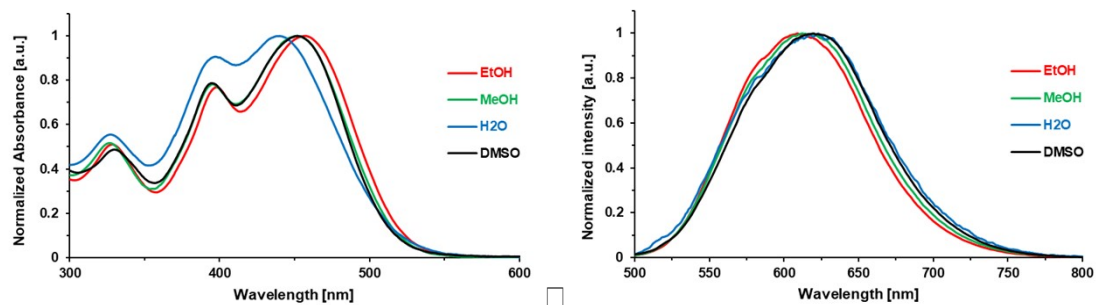
**Fig. S9**  $^1\text{H}$  NMR spectra of **5c** ( $\text{CDCl}_3$ ).



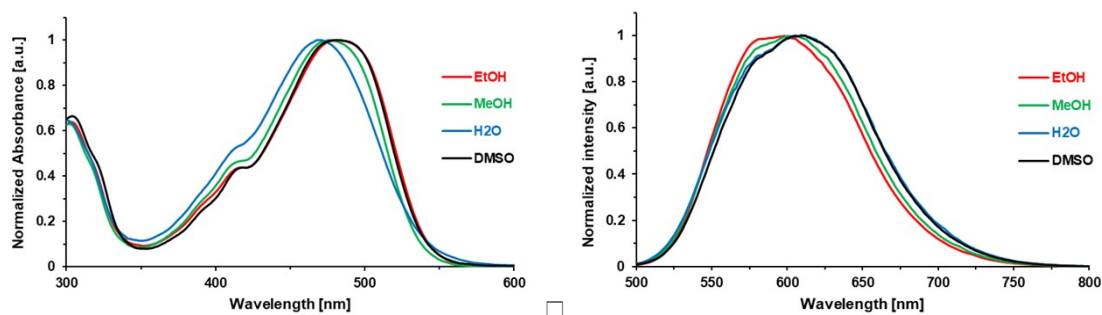


#### 4. Optical properties of 13PY, 16PY, and 18PY in solvents of different polarity.

##### 13PY



##### 16PY



##### 18PY

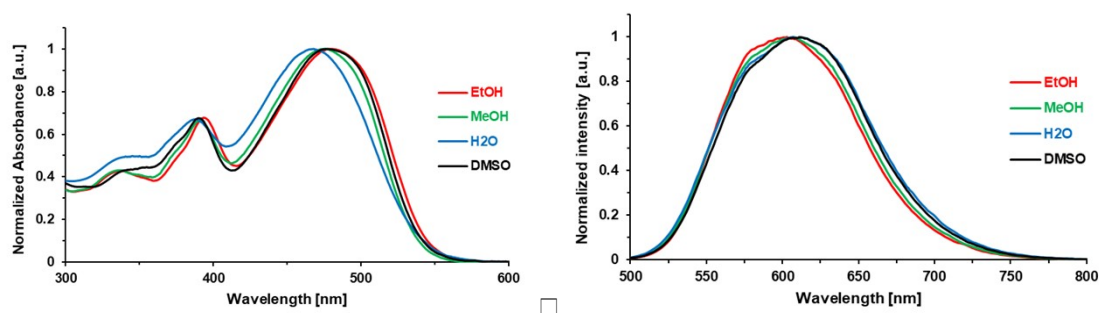


**Fig. S13** Absorption and fluorescence spectra of 13PY, 16PY, and 18PY in organic solvents of different polarity ( $\lambda_{\text{ex}} = \lambda_{\text{abs,max}}$ ).

**Table S1.** Spectroscopic properties of 13PY, 16PY, and 18PY.

Solvent	$\lambda_{\text{abs,max}} / \text{nm}$			$\lambda_{\text{fl}} / \text{nm}$			$\Phi$		
	13PY	16PY	18PY	13PY	16PY	18PY	13PY	16PY	18PY
DMSO	452	480	477	624	619	616	0.72	0.82	0.76
EtOH	457	483	481	609	598	603	0.53	0.62	0.53
MeOH	452	477	474	612	600	607	0.48	0.60	0.56
H <sub>2</sub> O	440	470	467	623	612	607	0.10	0.31	0.24

## 5. Confirmation of selective staining of 13PY, 16PY and 18PY into mitochondria in HEK293 cells.

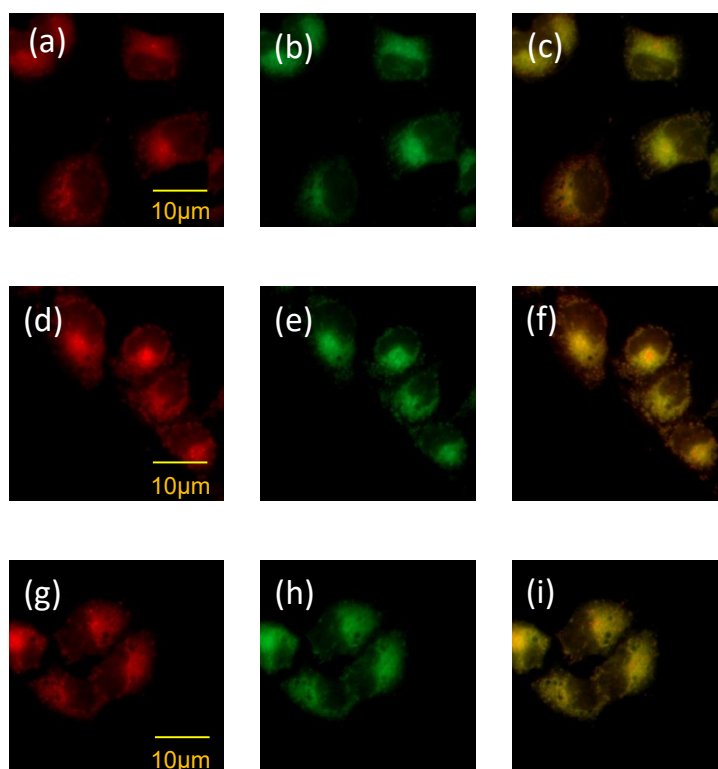


**Fig. S14** Single-photon fluorescence microscope images of HEK293 cells. (a), (d) and (g) are microscope image of cells stained with 13PY, 16PY, and 18PY, respectively. (b), (e) and (h) shows cells stained with MitoBright Green. (c), (f) and (i) are a merged image of (a) and (b), (d) and (e), (g) and (h).

**6. Time-lapse imaging of HEK293 cells stained with 13PY and 18PY after treatment with CCCP.**

**13PY**

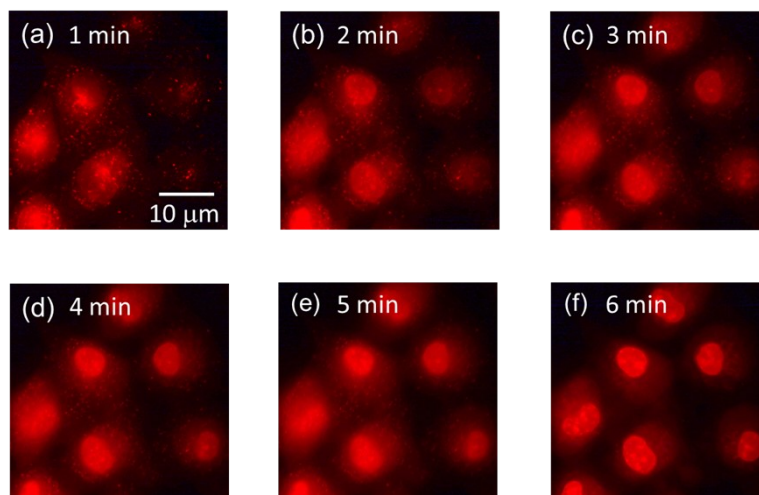


**Fig. S15** Single-photon fluorescence microscope images of HEK293 cells stained with 13PY after treatment with CCCP.

**18PY**

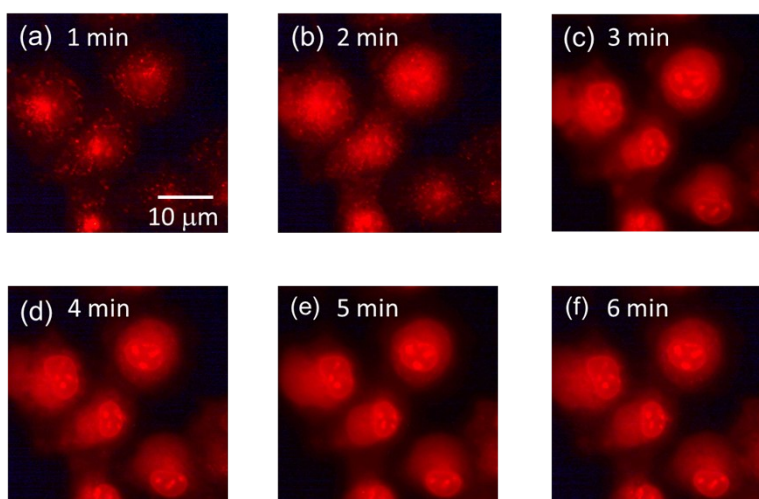


**Fig. S16** Single-photon fluorescence microscope images of HEK293 cells stained with 18PY after treatment with CCCP.

## 7. Confirmation of selective staining of 13PY and 18PY into nucleus after treatment with CCCP.

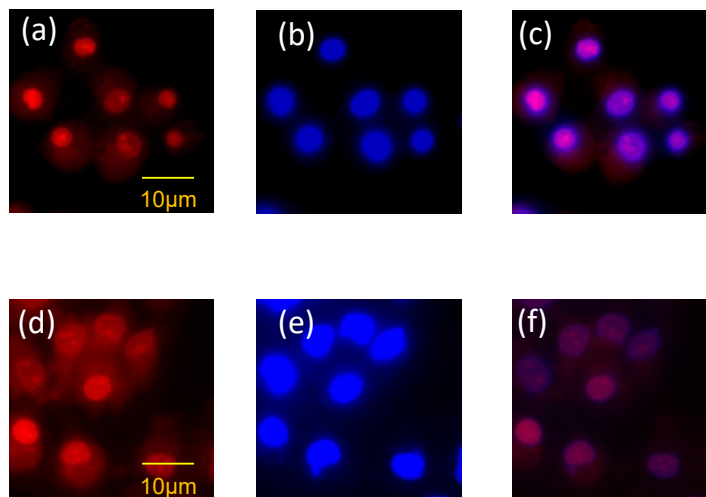


**Fig. S17** Single-photon fluorescence microscope images of HEK293 cells under reduced MMP condition. (a) and (d) are microscope image of cells stained with 13PY, and 18PY, respectively. (b), (e) and shows cells stained with Hoechst 33342. (c) and (f) are a merged image of (a) and (b), (d) and (e).

## 8. Cytotoxicity of 13PY, 16PY, and 18PY.

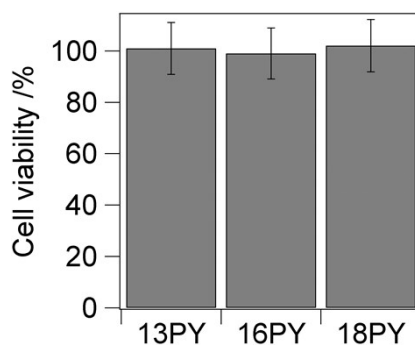


**Fig. S18** Cell viabilities after incubation with 13, 16, 18PY (1 µM) for 24h. This experiments were performed using Cell Counting Kit-8 (DOJINDO) according manufactures protocol.

## 9. Optical properties of 13PY, 16PY, 18PY, and PY-N in the presence of ctDNA.

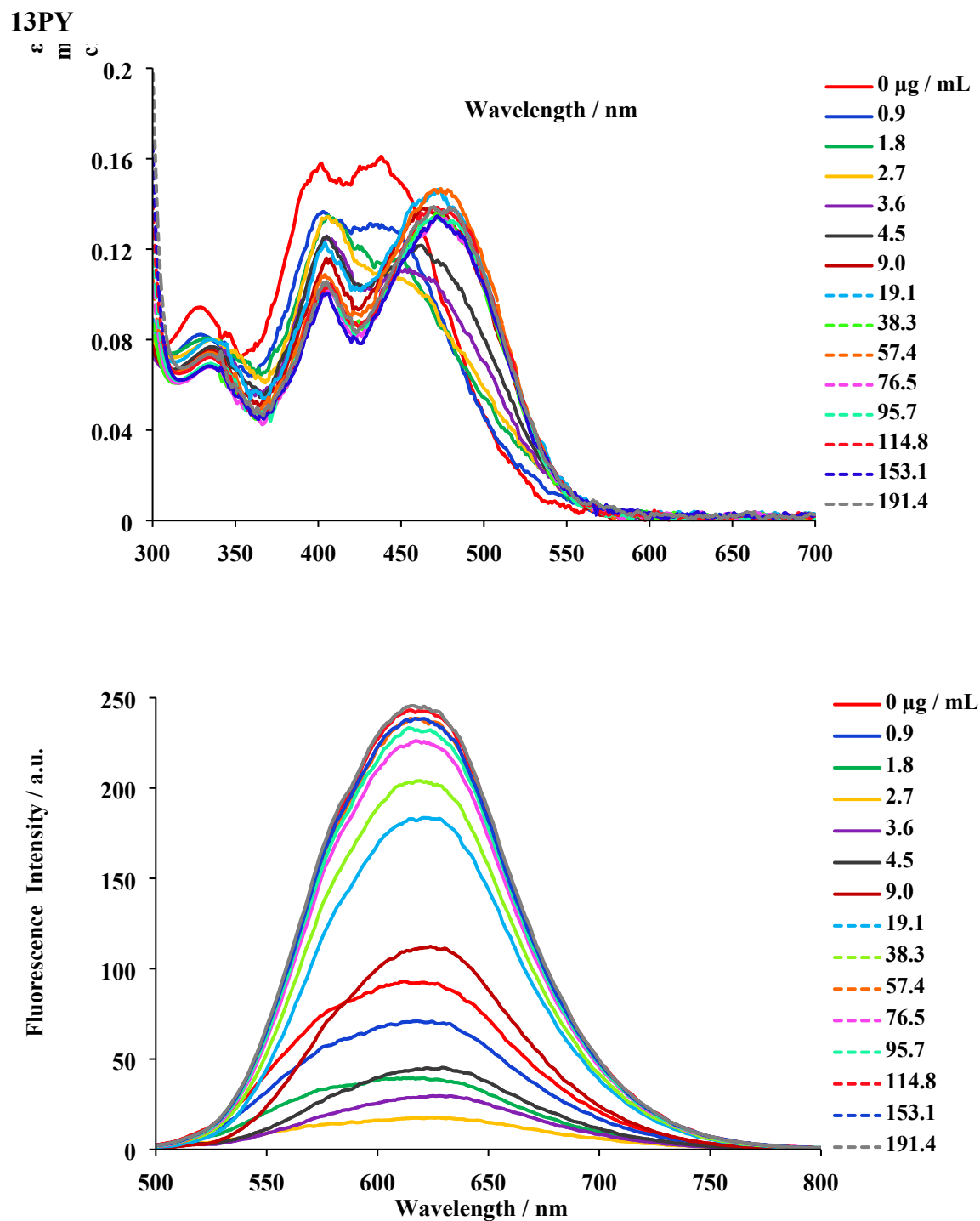
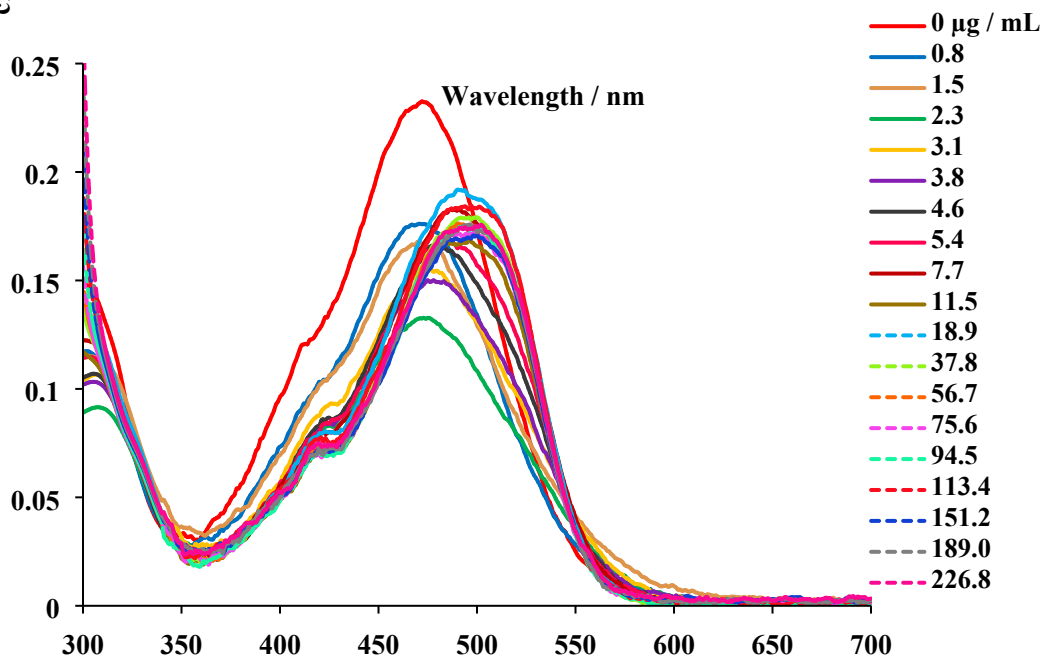


**Fig. S19** Absorption and fluorescence spectra of 13PY (5  $\mu\text{M}$ ) in presence of ctDNA. Excitation wavelength was 440 nm.

### 16PY

$\epsilon / \text{mol cm}^{-1}$



Fluore  
Inte  
/ a

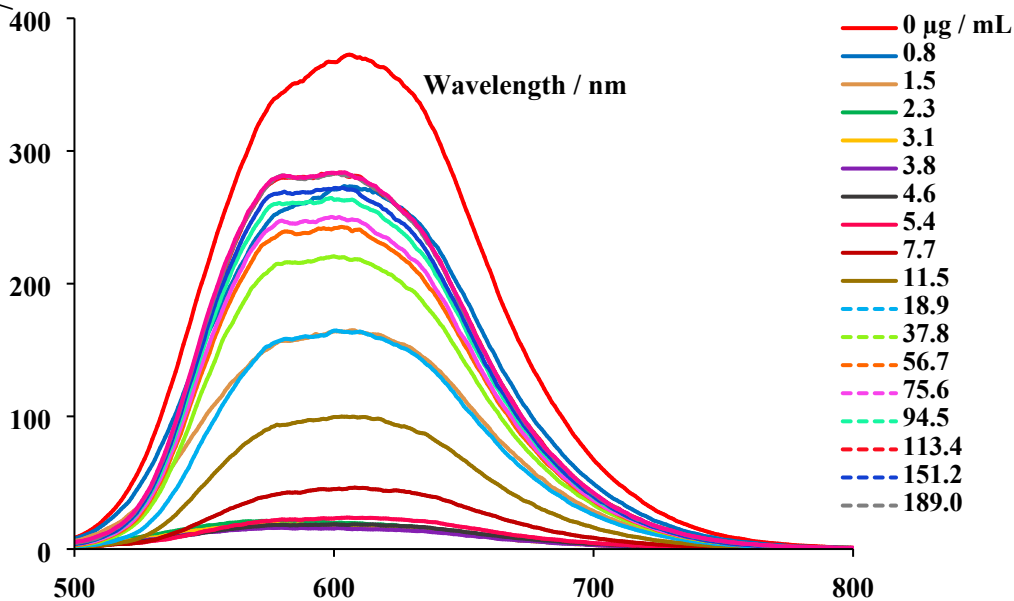


**Fig. S20** Absorption and fluorescence spectra of 16PY (5  $\mu\text{M}$ ) in presence of ctDNA. Excitation wavelength was 440 nm.

### 18PY

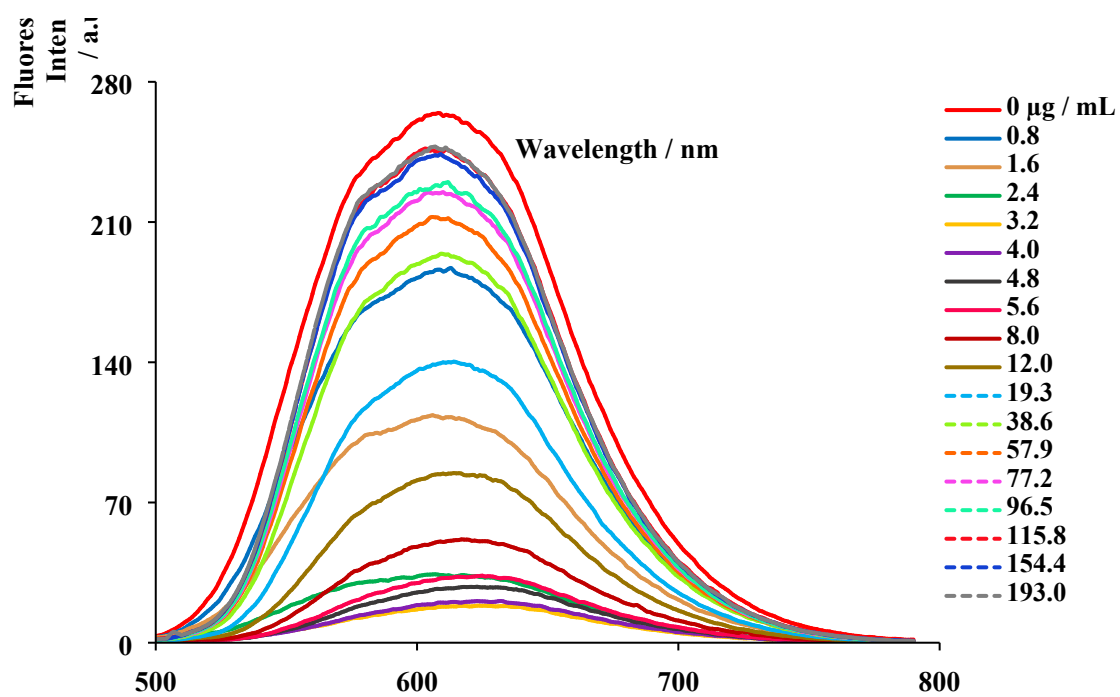
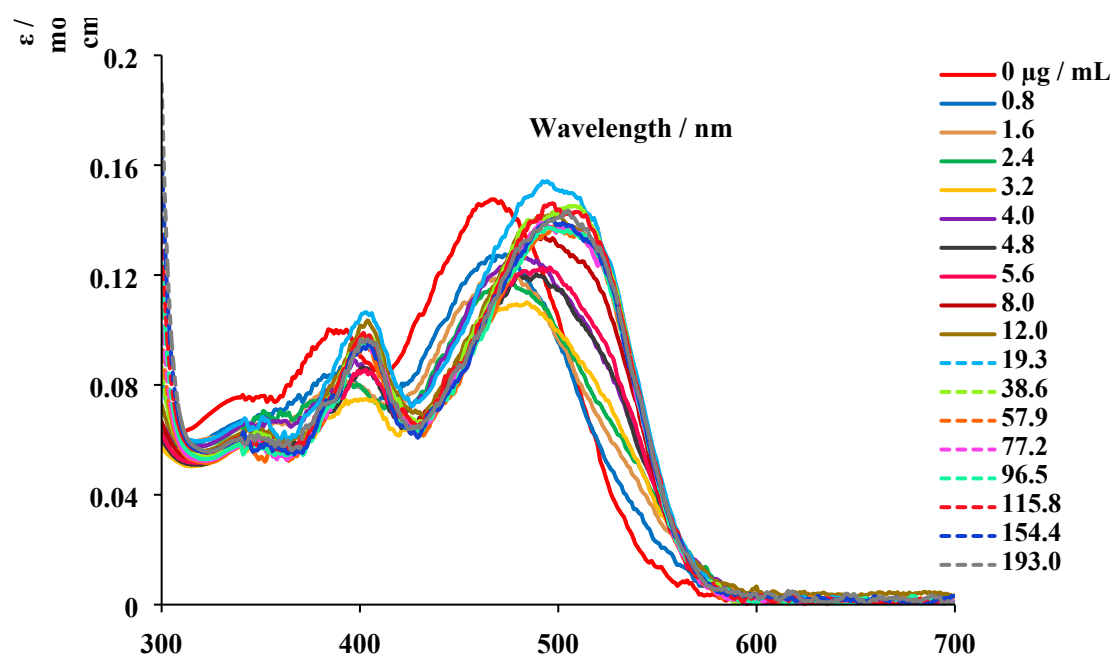


**Fig. S21** Absorption and fluorescence spectra of 18PY (5  $\mu\text{M}$ ) in presence of ctDNA. Excitation wavelength was 440 nm.

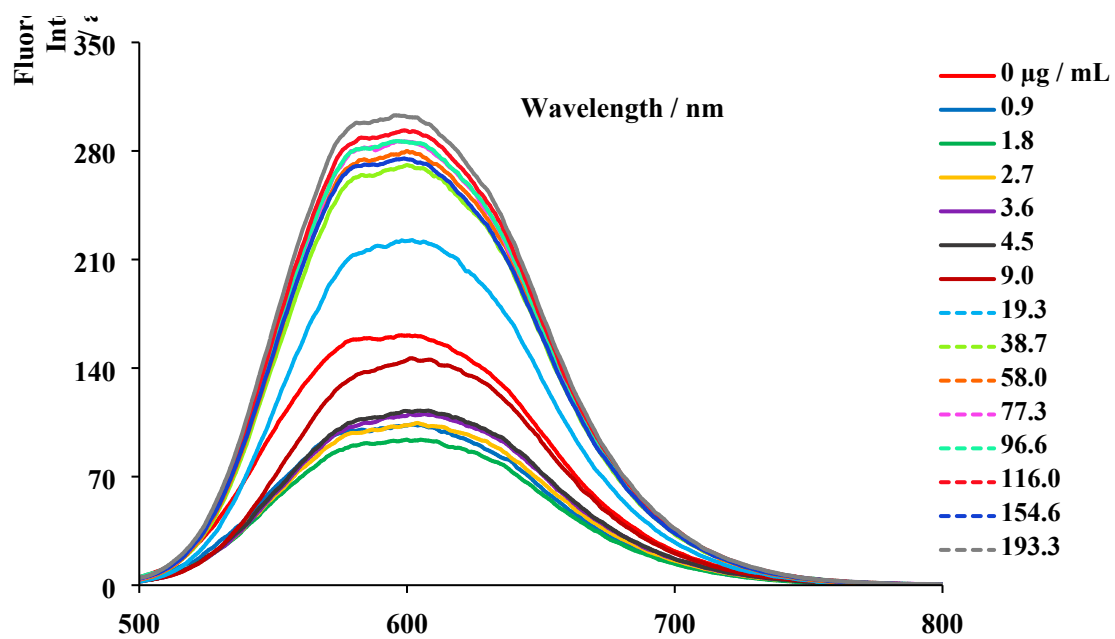
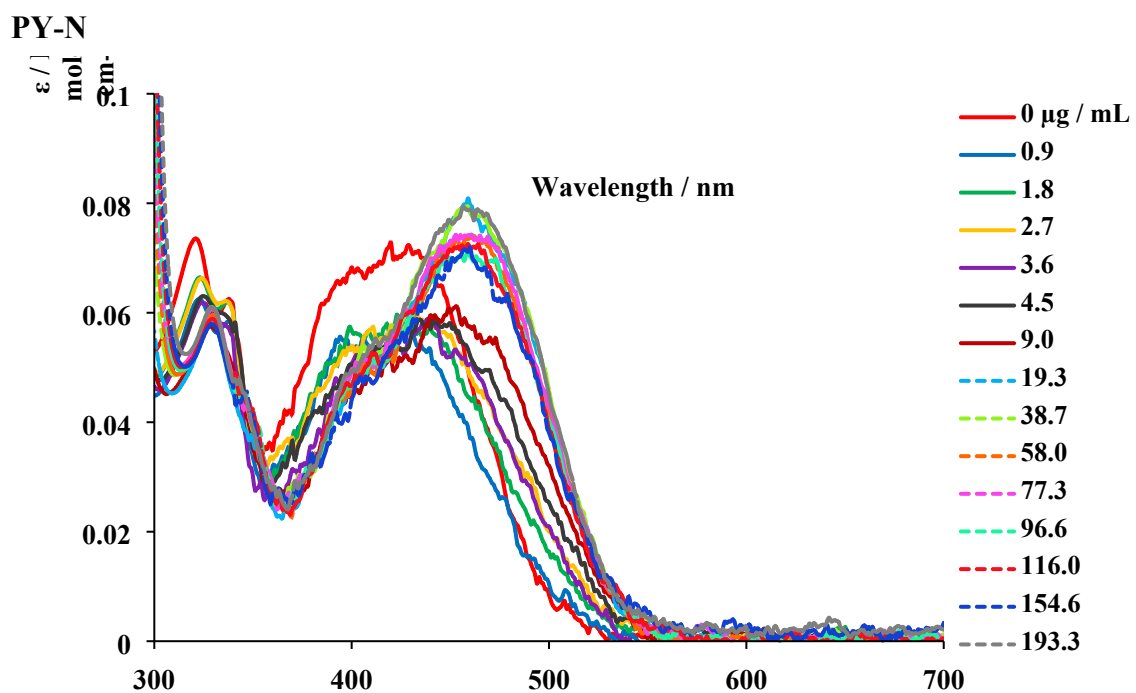


**Fig. S22** Absorption and fluorescence spectra of PY-N ( $5 \mu\text{M}$ ) in presence of ctDNA. Excitation wavelength was 450 nm.

**10. Time dependence of absorption and fluorescence spectra of 13PY, 16PY, 18PY, and PY after adding ctDNA.**

**13PY**

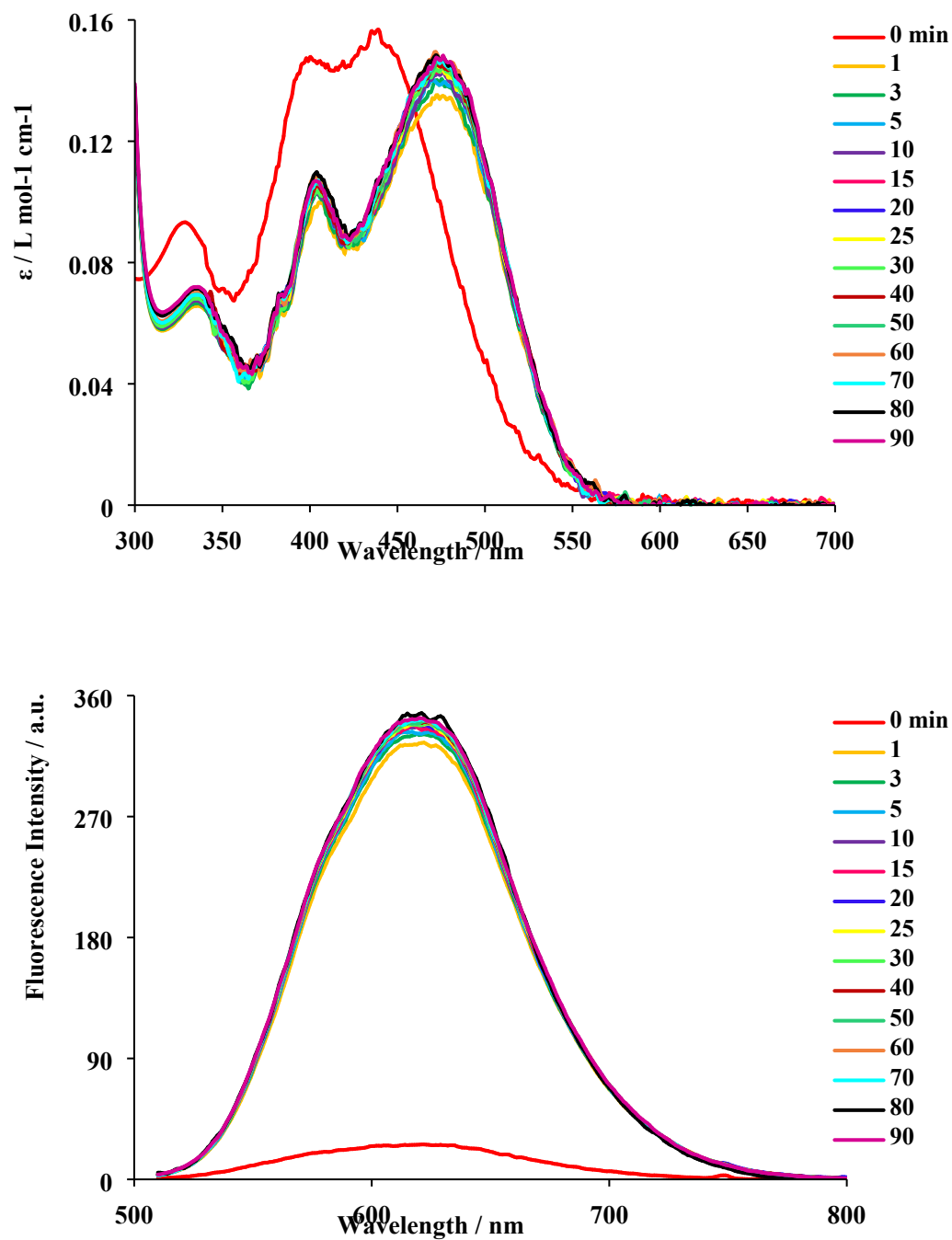


**Fig. S23** Time dependence of absorption and fluorescence spectra of 13PY (5  $\mu\text{M}$ ) after adding 100  $\mu\text{g/mL}$  of ctDNA. Excitation wavelength was 500 nm.

## 16PY

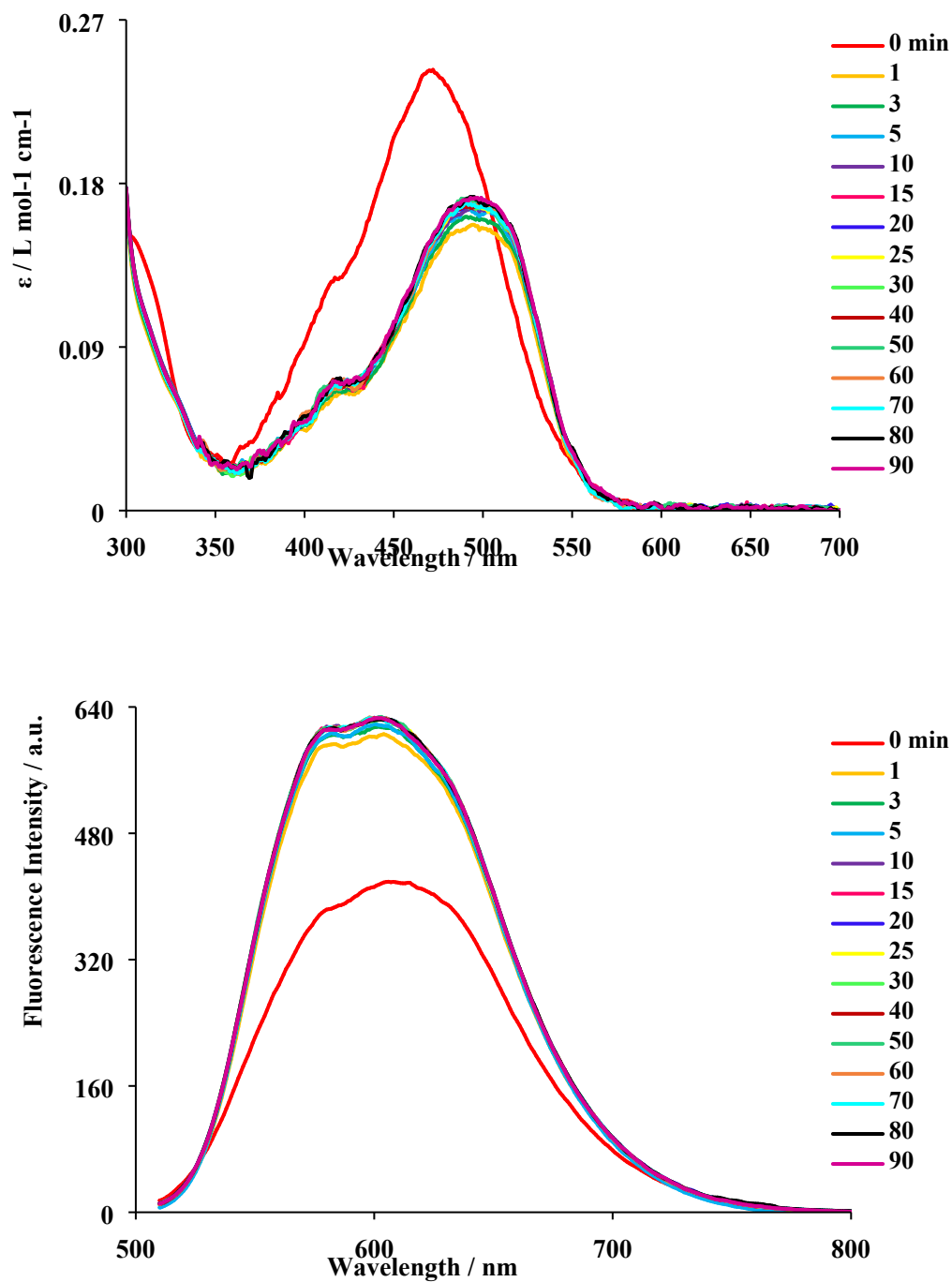


**Fig. S24** Time dependence of absorption and fluorescence spectra of 16PY (5  $\mu\text{M}$ ) after adding 100  $\mu\text{g/mL}$  of ctDNA. Excitation wavelength was 500 nm.

## 18PY

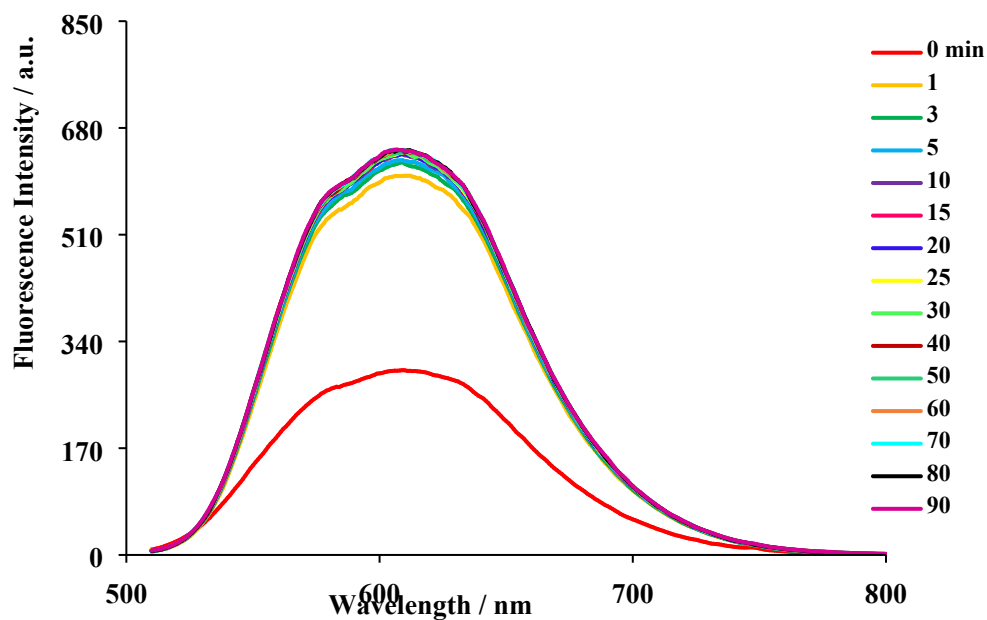
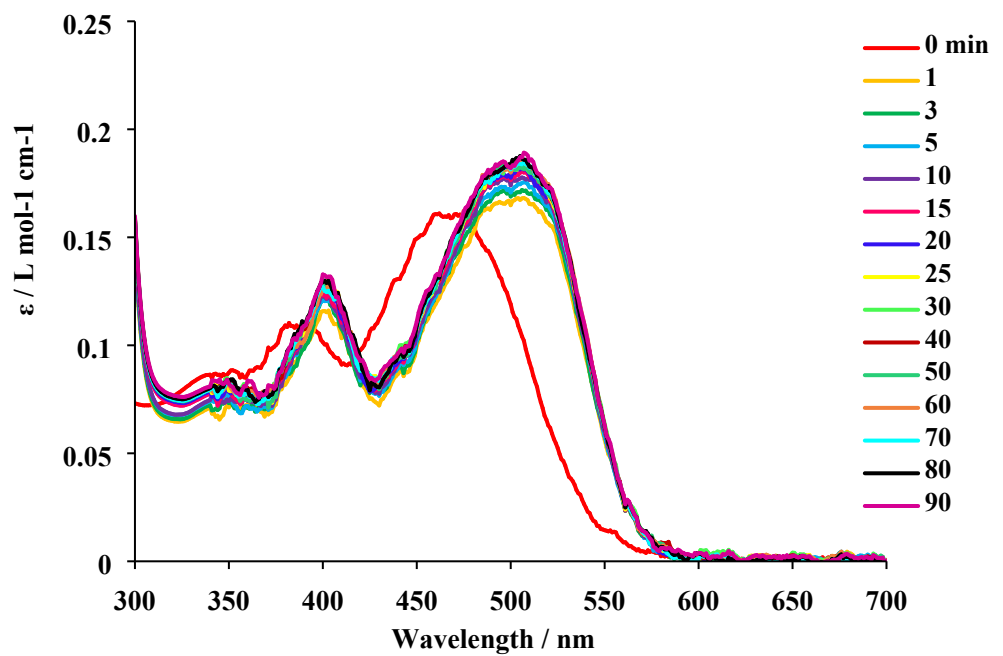


**Fig. S25** Time dependence of absorption and fluorescence spectra of 18PY (5  $\mu\text{M}$ ) after adding 100  $\mu\text{g/mL}$  of ctDNA. Excitation wavelength was 500 nm.

PY

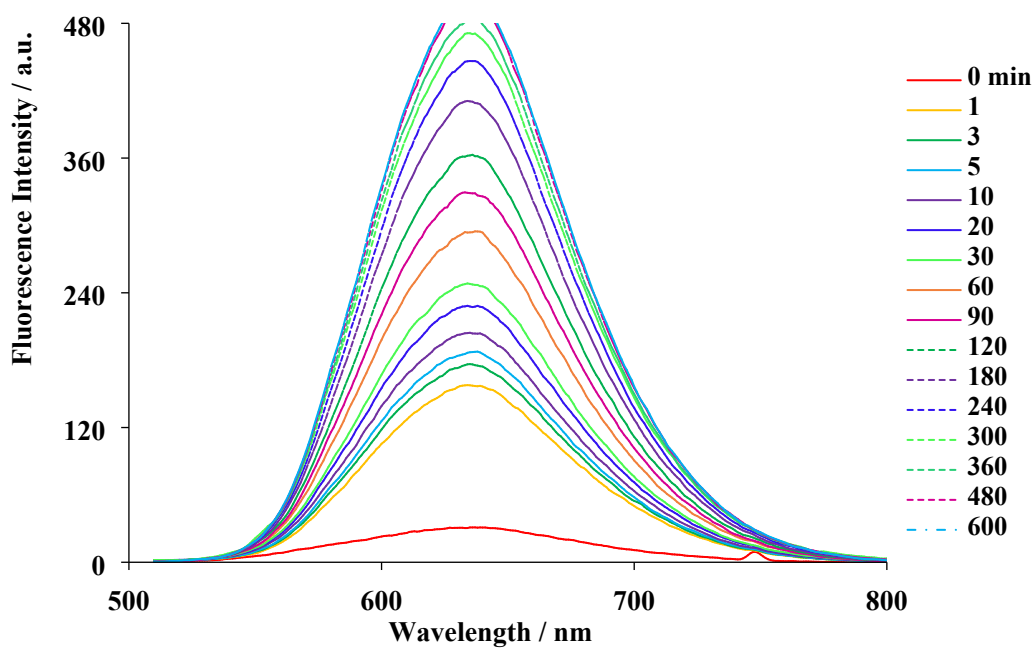
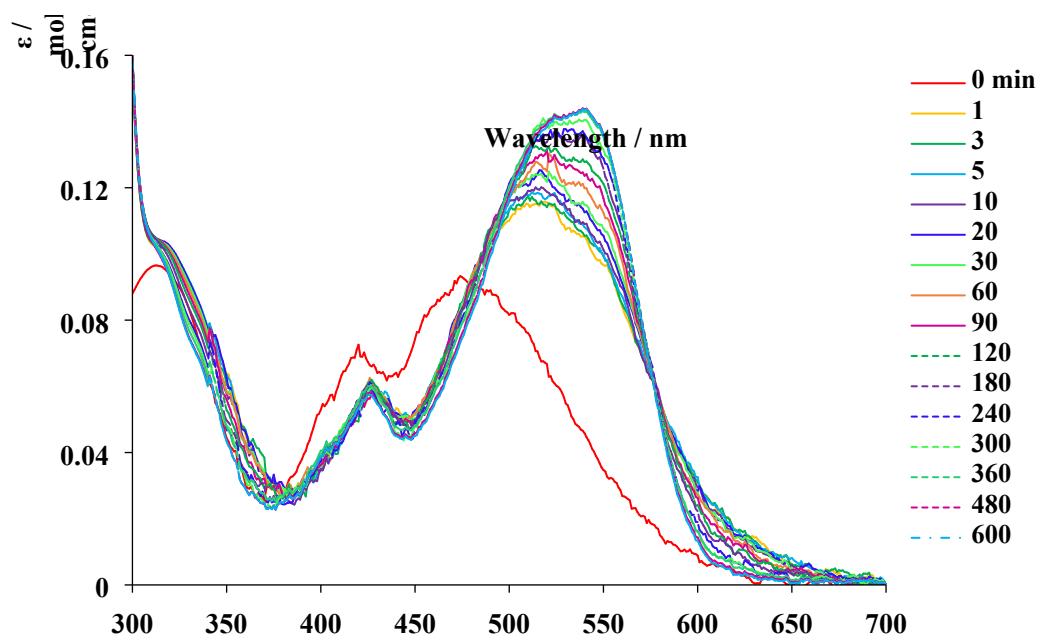


**Fig. S26** Time dependence of absorption and fluorescence spectra of PY (5  $\mu\text{M}$ ) after adding 100  $\mu\text{g/mL}$  of ctDNA. Excitation wavelength was 500 nm.

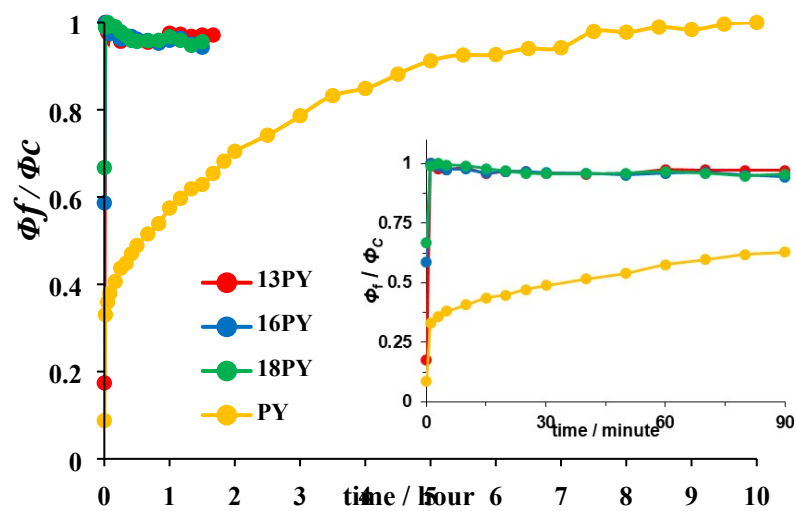


**Fig. S27** Time dependence of fluorescence quantum yield of 13PY, 16PY, 18PY, and PY (5  $\mu$ M) after adding 100  $\mu$ g/mL of ctDNA.

## 11. Optical properties of 13PY, 16PY, 18PY, and PY in the presence of liposomes.

### 13PY

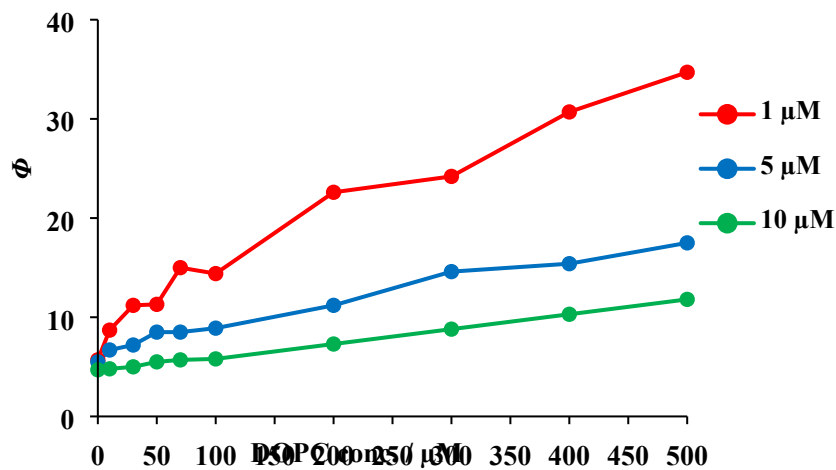


**Fig. S28** Dependence of the fluorescence quantum yield of 1-10  $\mu\text{M}$  13PY on the concentration of liposomes.  $\lambda_{\text{ex}} = 440 \text{ nm}$ .

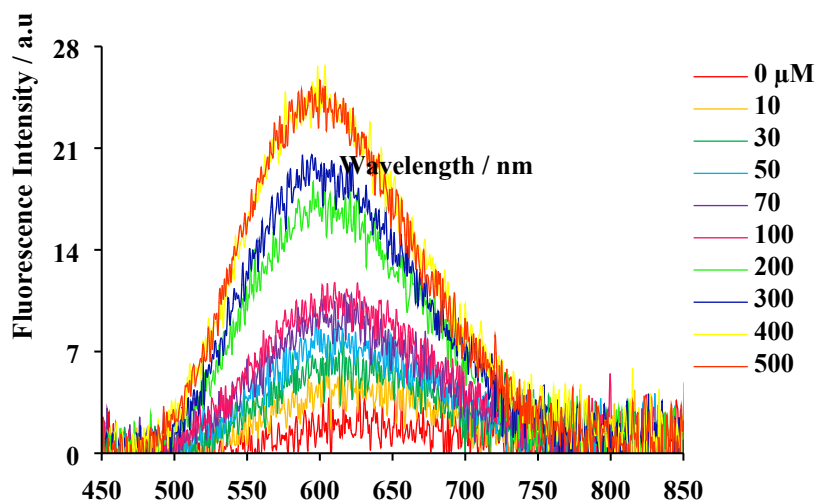


**Fig. S29** Fluorescence spectra of 13PY (1  $\mu\text{M}$ ) in presence of 0-500  $\mu\text{M}$  of liposomes. Excitation wavelength was 440 nm.

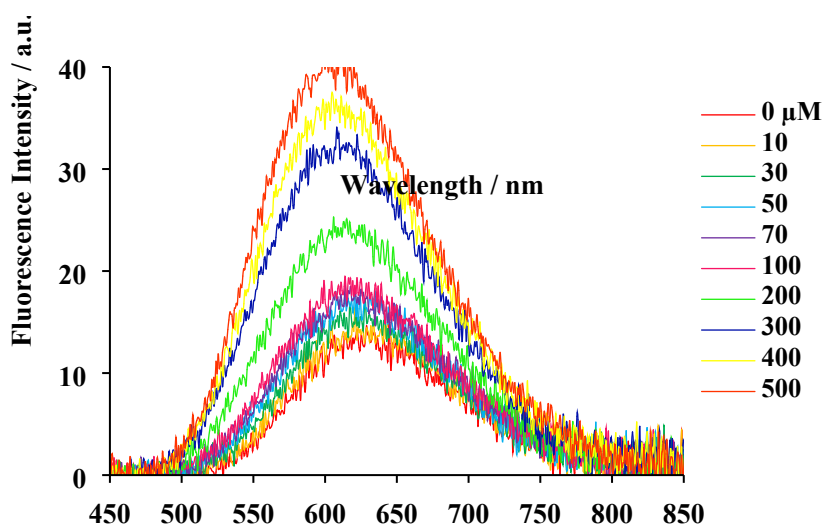


**Fig. S30** Fluorescence spectra of 13PY (5  $\mu\text{M}$ ) in presence of 0-500  $\mu\text{M}$  of liposomes. Excitation wavelength was 440 nm.

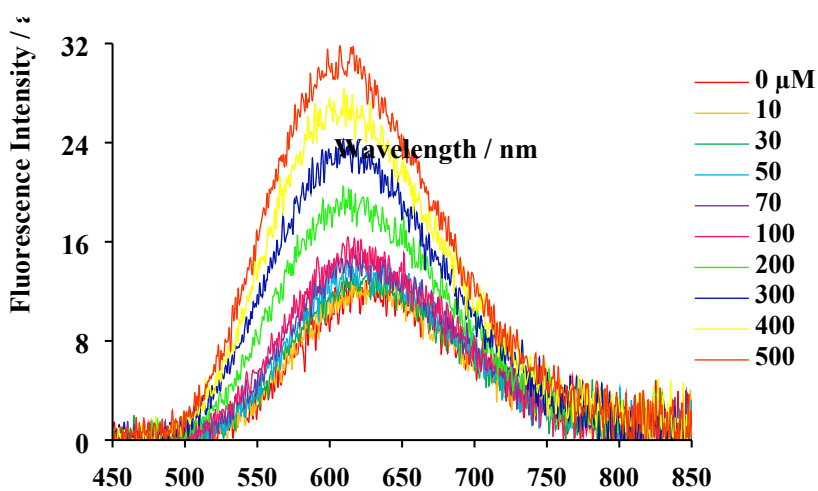


**Fig. S31** Fluorescence spectra of 13PY (10  $\mu\text{M}$ ) in presence of 0-500  $\mu\text{M}$  of liposomes. Excitation wavelength was 440 nm.

### 16PY

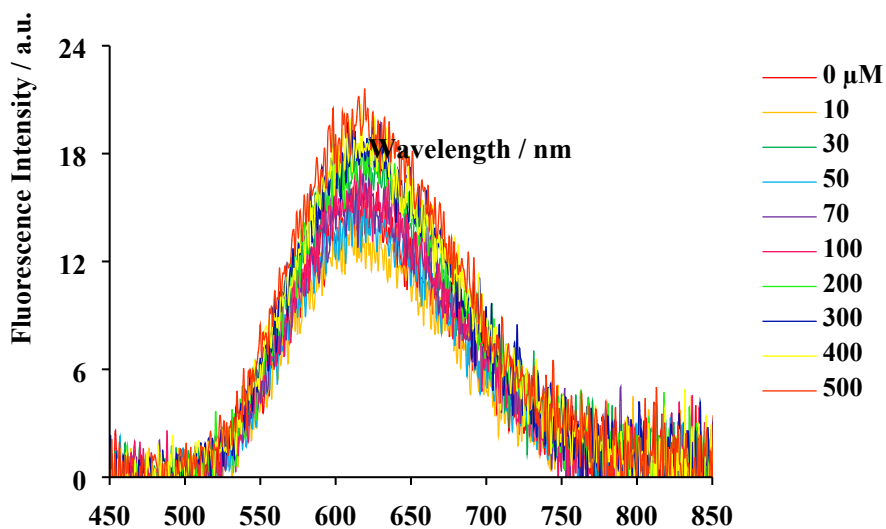


**Fig. S32** Fluorescence spectra of 16PY (1  $\mu\text{M}$ ) in presence of 0-500  $\mu\text{M}$  of liposomes. Excitation wavelength was 440 nm.

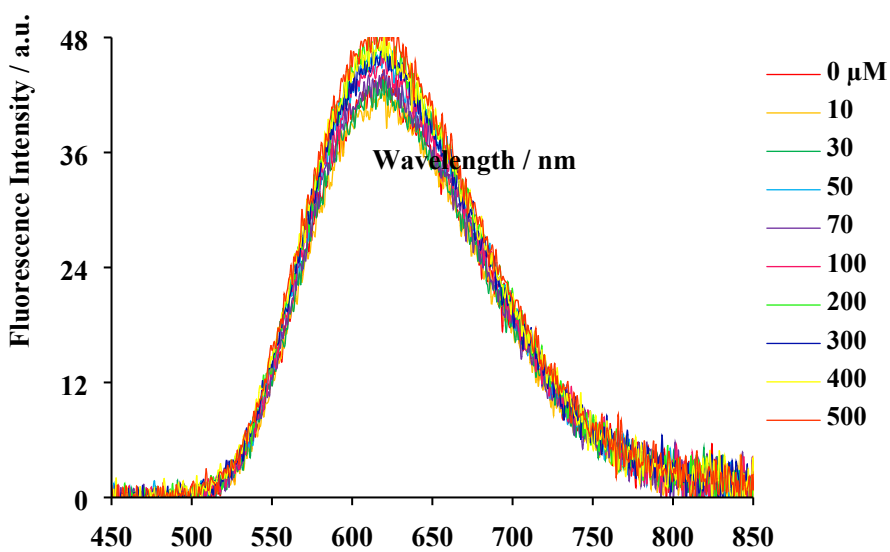


**Fig. S33** Fluorescence spectra of 16PY (5  $\mu\text{M}$ ) in presence of 0-500  $\mu\text{M}$  of liposomes. Excitation wavelength was 440 nm.

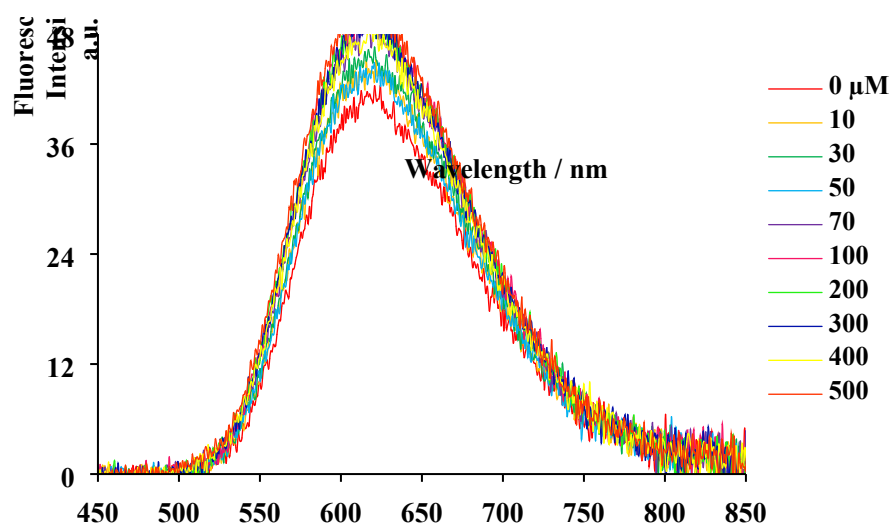


**Fig. S34** Fluorescence spectra of 16PY (10 μM) in presence of 0-500 μM liposomes. Excitation wavelength was 440 nm.

### 18PY

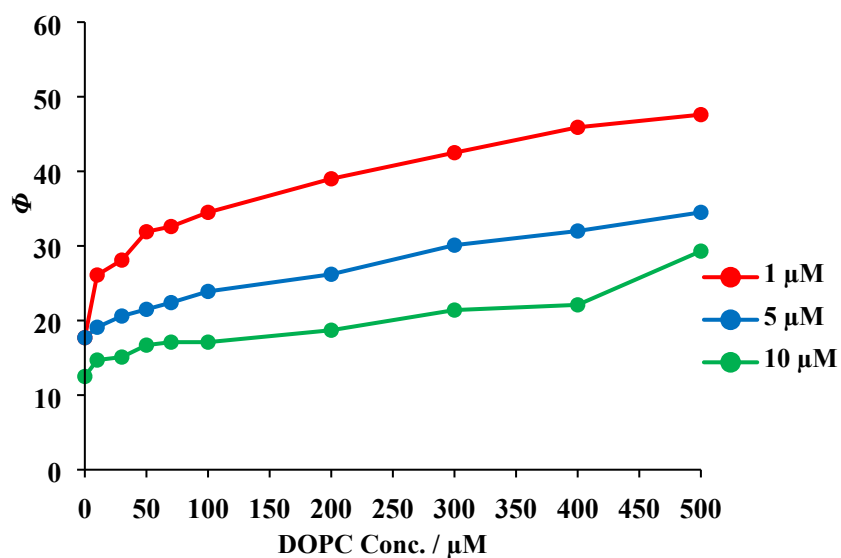


**Fig. S35** Dependence of the fluorescence quantum yield of 1-10  $\mu\text{M}$  18PY on the concentration of liposomes.

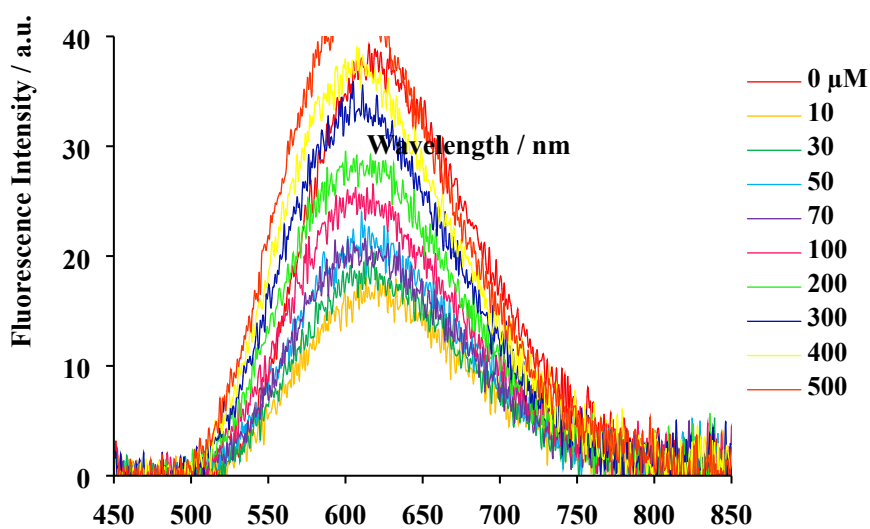


**Fig. S36** Fluorescence spectra of 18PY (1  $\mu\text{M}$ ) in presence of 0-500  $\mu\text{M}$  of liposomes. Excitation wavelength was 440 nm.

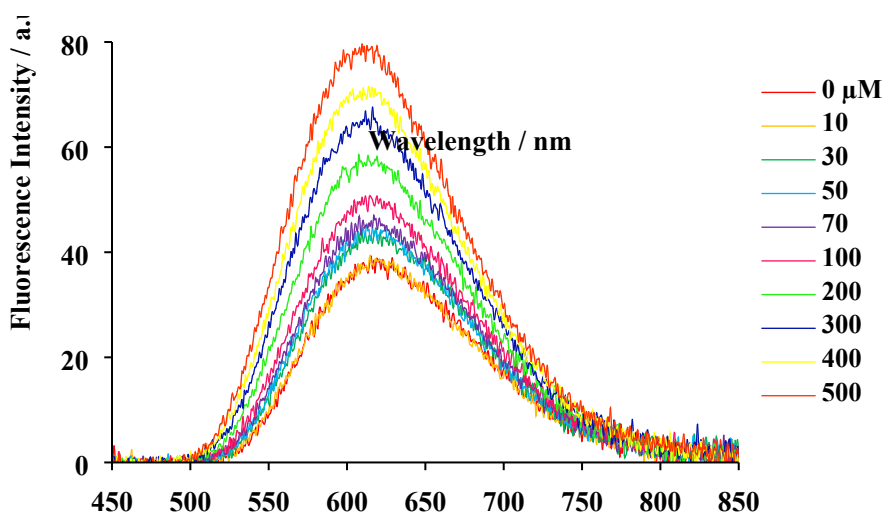


**Fig. S37** Fluorescence spectra of 18PY (5  $\mu\text{M}$ ) in presence of 0-500  $\mu\text{M}$  of liposomes. Excitation wavelength was 440 nm.

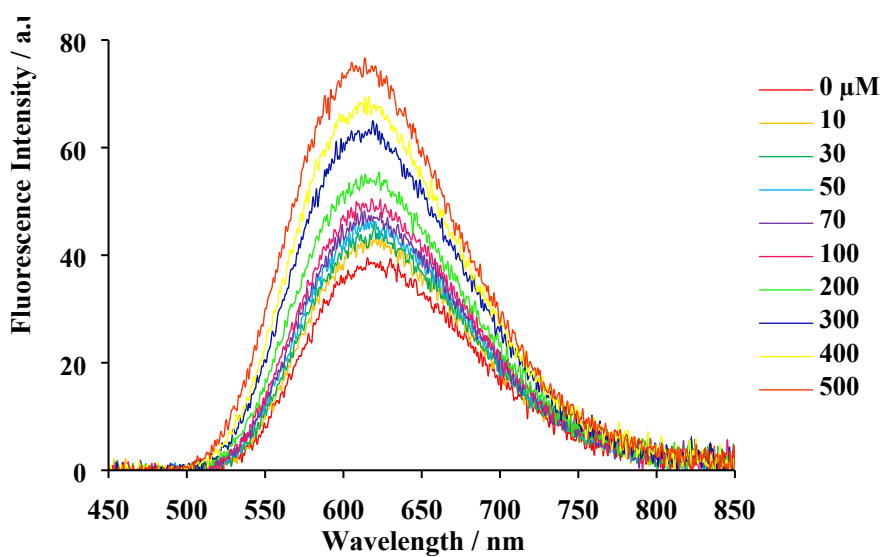


**Fig. S38** Fluorescence spectra of 18PY (10  $\mu\text{M}$ ) in presence of 0-500  $\mu\text{M}$  of liposomes. Excitation wavelength was 440 nm.

PY

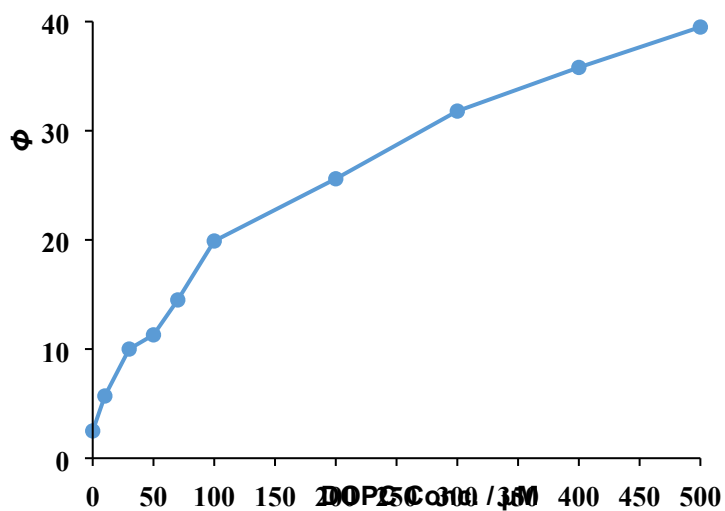


**Fig. S39** Dependence of the fluorescence quantum yield of PY ( $5 \mu\text{M}$ ) on the concentration of liposomes.

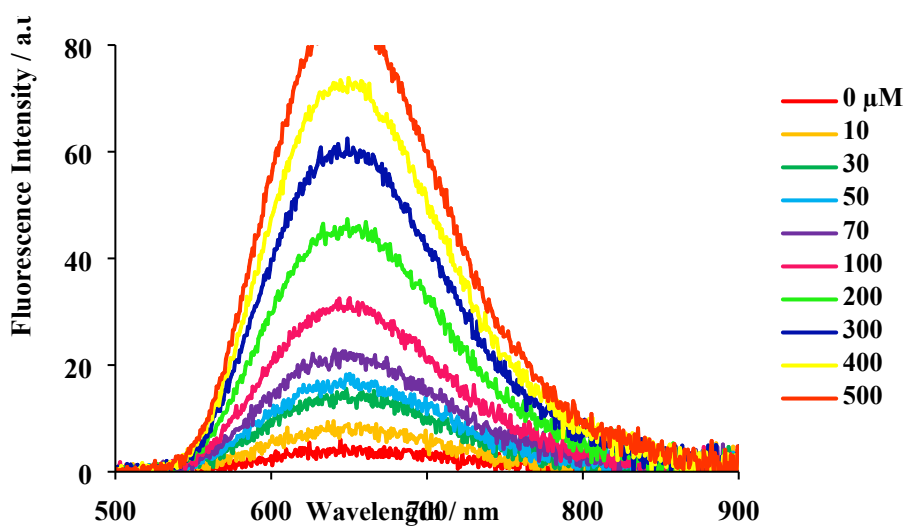
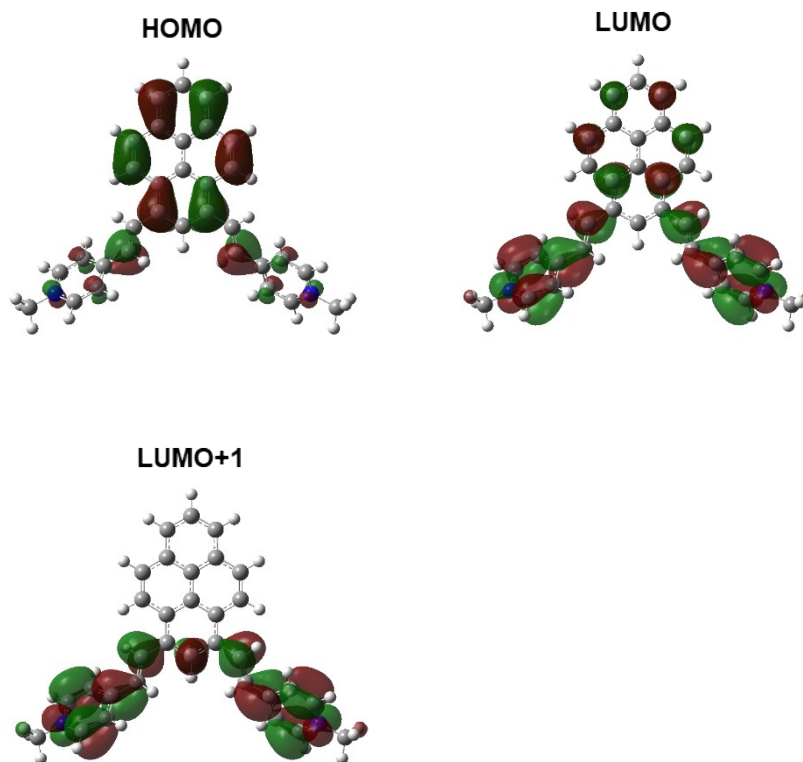


**Fig. S40** Fluorescence spectra of PY ( $5 \mu\text{M}$ ) in presence of 0-500  $\mu\text{M}$  of liposomes. Excitation wavelength was 480 nm.

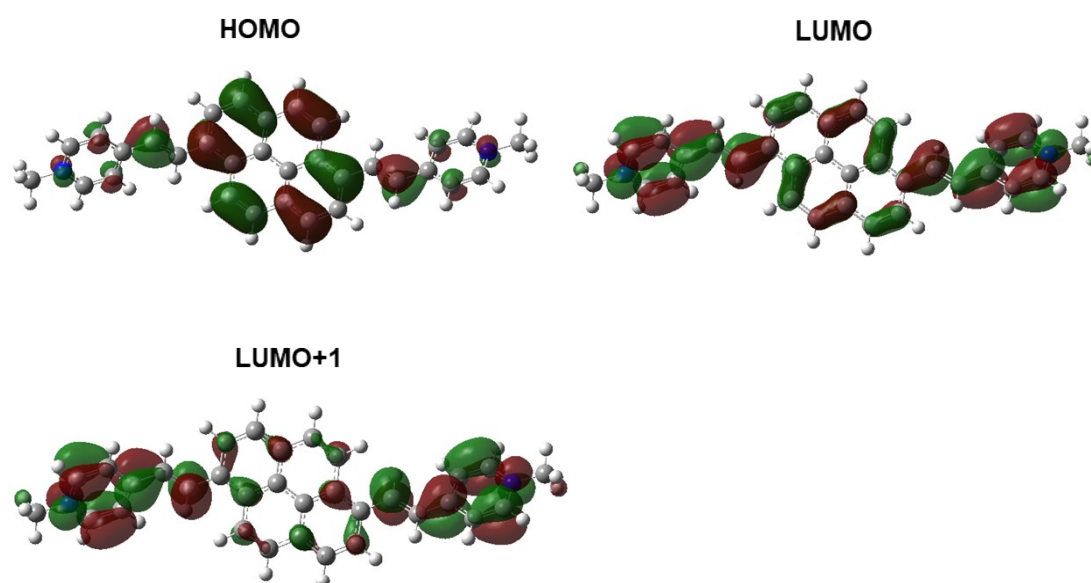
## 12. DFT calculation.

Molecular orbitals of 13PY, 16PY, and 18PY.

13PY



16PY



18PY

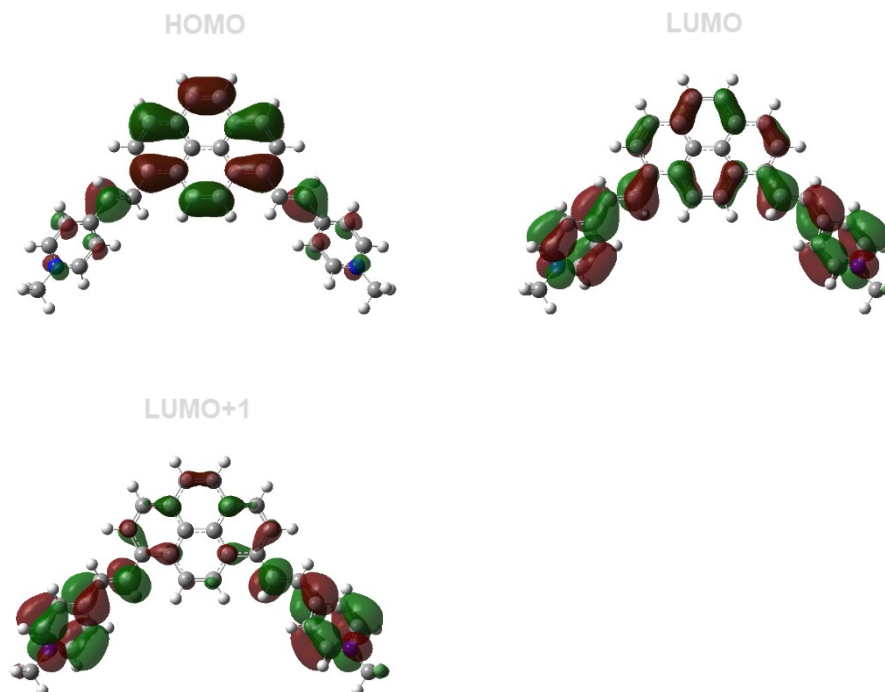


**Fig. S41** The MOs of 13PY, 16PY, and 18PY used in this work.

**Table S2.** Excitation energy, osillator strength ( $f_e$ ), main transition orbital calculated for **13PY**, **16PY** and **18PY** using TD-DFT (M062X/6-31+G(d,p)).

Entry	State	Excitation energy [eV]	$f_e$	Main transition orbital	Contribution
<b>13PY</b>	S1	2.53	0.60	HOMO→LUMO+1	
	S2	2.56	0.80	HOMO→LUMO	
	S3	3.34	0.20	HOMO-2→LUMO	0.88
				HOMO-2→LUMO+4	0.07
				HOMO→LUMO+5	0.05
	S4	3.73	0.03	HOMO-1→LUMO+1	0.95
				HOMO→LUMO+4	0.05
	S5	4.00	0.24	HOMO-4→LUMO+1	0.05
				HOMO-3→LUMO	0.84
HOMO-2→LUMO+4				0.08	
HOMO-1→LUMO+4				0.03	

<b>16PY</b>	S1	2.50	1.73	HOMO-2→LUMO+1	0.03	
				HOMO→LUMO	0.97	
	S2	2.95	0.00	HOMO→LUMO+1	05	
	S3	3.40	0.15	HOMO-1→LUMO	0.84	
				HOMO-1→LUMO+4	0.06	
				HOMO→LUMO+5	0.10	
	S4	3.84	0.00	HOMO-3→LUMO	0.03	
				05		
				HOMO-2→LUMO	0.32	
	S5	4.11	0.00	HOMO-1→LUMO+1	0.65	
				HOMO-3→LUMO	0.21	
				02		
				HOMO-3→LUMO+4	0.04	
				HOMO-2→LUMO	0.42	
				HOMO-1→LUMO+1	0.33	
<b>18PY</b>	S1	2.44	1.22	HOMO→LUMO		
	S2	2.91	0.37	HOMO→LUMO+1		
	S3	3.34	0.27	HOMO-4→LUMO+1	0.03	
				HOMO-1→LUMO	0.88	
				HOMO-1→LUMO+4	0.04	
				HOMO→LUMO+5	0.05	
	S4	3.78	0.13	HOMO-4→LUMO	0.06	
				HOMO-2→LUMO	0.08	
				HOMO-1→LUMO+1	0.84	
				HOMO→LUMO	0.02	
	S5	4.08	0.01	HOMO-2→LUMO	0.66	
				HOMO-2→LUMO+4	0.08	
HOMO-1→LUMO+1				0.09		
HOMO→LUMO+4				0.17		

**Atom coordinates and absolute energies of pyrene derivatives in ground states.**

**Table S3.** Atom coordinates and absolute energies of **13PY**, **16PY** and **18PY** in theoretical calculations.

		13PY (ground): E(RM062X) = -1343.58871566			A.U.
Center number	Atomic number	Coordinates (Angstroms)			
		X	Y	Z	
1	6	0.000038	6.812166	-0.000015	
2	6	-1.204634	6.116891	-0.019914	
3	6	-1.22332	4.714872	-0.023087	
4	6	0.00002	3.995808	-0.00001	
5	6	1.223369	4.714856	0.023065	
6	6	1.204701	6.116875	0.019886	
7	6	-2.44957	3.977577	-0.035638	
8	6	0.00001	2.566174	-0.000006	
9	6	-1.238373	1.861548	-0.050434	
10	6	-2.457693	2.617072	-0.042572	
11	6	-1.222018	0.437075	-0.066297	
12	6	-0.000003	-0.23432	0.00001	
13	6	1.222016	0.437065	0.066303	
14	6	1.238384	1.861535	0.050426	
15	6	2.457715	2.617041	0.042567	
16	6	2.44961	3.977545	0.035625	
17	1	3.38613	4.528277	0.029201	
18	1	3.411204	2.10347	0.014646	
19	1	-3.386083	4.528319	-0.029211	
20	1	0.000045	7.896625	-0.000017	
21	1	-2.146189	6.658649	-0.032918	
22	1	2.146263	6.658621	0.032891	
23	1	-3.411191	2.103518	-0.014637	
24	1	-0.000008	-1.32089	0.000022	
25	6	-2.467964	-0.31207	-0.175016	
26	1	-3.279478	0.195984	-0.690889	
27	6	2.467963	-0.31208	0.175027	
28	1	3.279551	0.196077	0.69068	
29	6	-2.701942	-1.55062	0.316717	
30	1	-1.948967	-2.04465	0.925881	

31	6	2.701878	-1.55071	-0.316538
32	1	1.948816	-2.04484	-0.925517
33	6	-3.965119	-2.25154	0.170654
34	6	-4.244217	-3.37293	0.980229
35	6	-4.969298	-1.87889	-0.749032
36	6	-5.449078	-4.02841	0.884094
37	1	-3.517184	-3.72784	1.702114
38	6	-6.157451	-2.56781	-0.802001
39	1	-4.825748	-1.06347	-1.44723
40	1	-5.700035	-4.88447	1.500116
41	1	-6.95055	-2.30617	-1.493275
42	6	3.965074	-2.25161	-0.170545
43	6	4.244077	-3.37309	-0.980044
44	6	4.969364	-1.87887	0.748984
45	6	5.448954	-4.02854	-0.883998
46	1	3.516955	-3.72807	-1.701801
47	6	6.157527	-2.56777	0.80187
48	1	4.825901	-1.06339	1.447118
49	1	5.699841	-4.88466	-1.499968
50	1	6.950714	-2.30606	1.493014
51	6	7.699442	-4.31708	0.037972
52	1	7.546106	-5.37718	-0.159337
53	1	8.132003	-4.1946	1.029537
54	1	8.362574	-3.88664	-0.714472
55	6	-7.699444	-4.31706	-0.038148
56	1	-7.546128	-5.37712	0.159342
57	1	-8.131841	-4.19473	-1.029803
58	1	-8.362703	-3.88652	0.714126
59	7	6.395143	-3.62591	-0.006414
60	7	-6.395159	-3.62587	0.006351

16PY (ground): E(RM062X) = -1343.59902069

A.U.

Center number	Atomic number	Coordinates (Angstroms)		
		X	Y	Z
1	6	2.790652	-2.1436	-0.11123
2	6	1.516541	-2.67693	-0.09207
3	6	0.393925	-1.83593	-0.08708
4	6	0.573639	-0.42804	-0.0989
5	6	1.888724	0.123064	-0.10693
6	6	3.0046	-0.75429	-0.11758
7	6	-0.93725	-2.3685	-0.06811
8	6	-0.57364	0.428033	-0.09902
9	6	-1.88873	-0.12307	-0.10688
10	6	-2.02362	-1.55476	-0.07039
11	6	-3.0046	0.754282	-0.11778
12	6	-2.79066	2.143593	-0.11181
13	6	-1.51655	2.67693	-0.09282
14	6	-0.39393	1.835927	-0.08761
15	6	0.937244	2.368508	-0.0688
16	6	2.023616	1.554764	-0.07086
17	1	3.009311	2.00289	-0.0224
18	1	1.061069	3.447157	-0.04166
19	1	-1.06107	-3.44715	-0.04065
20	1	3.64155	-2.81455	-0.16629
21	1	1.375652	-3.75354	-0.0998
22	1	-3.00932	-2.00287	-0.02179
23	1	-3.64156	2.814523	-0.16705
24	1	-1.37566	3.753534	-0.10084
25	6	4.369938	-0.24025	-0.17631
26	6	5.459973	-0.89609	0.283699
27	1	4.502898	0.740848	-0.62612
28	1	5.335359	-1.83743	0.812494
29	6	6.825681	-0.41672	0.176387
30	6	7.848974	-1.08006	0.886085
31	6	7.222019	0.683875	-0.61283
32	6	9.15161	-0.64757	0.811607
33	1	7.620288	-1.93849	1.507751

34	6	8.538855	1.076108	-0.64962
35	1	6.512324	1.233894	-1.21859
36	1	9.960589	-1.13349	1.34548
37	1	8.878047	1.915117	-1.24635
38	6	10.90412	0.833184	-0.04036
39	1	11.40813	0.224026	-0.7928
40	1	10.94835	1.884101	-0.32102
41	1	11.37879	0.699881	0.930872
42	7	9.489355	0.421649	0.056075
43	6	-4.36994	0.240217	-0.1764
44	6	-5.45998	0.896156	0.283465
45	1	-4.5029	-0.74098	-0.626
46	1	-5.33536	1.837607	0.812066
47	6	-6.82568	0.416757	0.176238
48	6	-7.84898	1.080175	0.885868
49	6	-7.22201	-0.68394	-0.61284
50	6	-9.15161	0.647653	0.811464
51	1	-7.62029	1.938682	1.507427
52	6	-8.53884	-1.0762	-0.64956
53	1	-6.51232	-1.23401	-1.21855
54	1	-9.96059	1.133617	1.345291
55	1	-8.87803	-1.91528	-1.24619
56	6	-10.9041	-0.83324	-0.04029
57	1	-11.4081	-0.22413	-0.79275
58	1	-10.9483	-1.88417	-0.32089
59	1	-11.3787	-0.69989	0.930948
60	7	-9.48934	-0.42167	0.056067

**18PY** (ground): E(RM062X) = -1343.59464135

A.U.

Center number	Atomic number	Coordinates (Angstroms)		
		X	Y	Z
1	6	3.515375	2.582942	0.125202
2	6	2.857577	1.34135	0.111395
3	6	1.43825	1.310181	0.063295
4	6	0.71519	2.535217	0.027478
5	6	1.412867	3.775389	0.044267
6	6	2.81389	3.772719	0.092555
7	6	0.679378	0.09111	0.022774
8	6	-0.71518	2.535211	-0.02748
9	6	-1.43823	1.310169	-0.06328
10	6	-0.67935	0.091104	-0.02274
11	6	-2.85756	1.341328	-0.11138
12	6	-3.51537	2.582914	-0.1252
13	6	-2.81389	3.772696	-0.09257
14	6	-1.41287	3.775377	-0.04428
15	6	-0.67779	5.007954	-0.02069
16	6	0.677774	5.007959	0.020668
17	1	1.232677	5.941163	0.037296
18	1	-1.2327	5.941154	-0.03733
19	1	1.194788	-0.86291	0.020552
20	1	4.596309	2.613344	0.213166
21	1	3.34596	4.718746	0.123392
22	1	-1.19475	-0.86292	-0.02051
23	1	-4.59631	2.613304	-0.21316
24	1	-3.34597	4.718719	-0.12341
25	6	-3.64996	0.118116	-0.18758
26	6	-4.92424	0.01059	0.256025
27	1	-3.1747	-0.75176	-0.63669
28	1	-5.3725	0.844436	0.789692
29	6	3.649976	0.11814	0.187606
30	6	4.924257	0.010599	-0.25602
31	1	3.174722	-0.75174	0.636719
32	1	5.372513	0.844431	-0.78971
33	6	-5.76767	-1.16102	0.119402

34	6	-6.99374	-1.21157	0.813549
35	6	-5.46	-2.27432	-0.69368
36	6	-7.82437	-2.30188	0.699265
37	1	-7.29935	-0.38997	1.451722
38	6	-6.32474	-3.33862	-0.77041
39	1	-4.5568	-2.30672	-1.29072
40	1	-8.77295	-2.37029	1.219462
41	1	-6.12664	-4.20688	-1.38918
42	6	5.76767	-1.16102	-0.1194
43	6	6.993729	-1.21159	-0.81357
44	6	5.460009	-2.27431	0.693703
45	6	7.824354	-2.3019	-0.69929
46	1	7.299339	-0.39	-1.45175
47	6	6.324735	-3.33862	0.770421
48	1	4.556818	-2.30669	1.29076
49	1	8.772916	-2.37033	-1.21951
50	1	6.126637	-4.20687	1.389198
51	6	-8.41023	-4.49737	-0.23447
52	1	-8.92984	-4.41743	-1.19082
53	1	-7.83701	-5.42311	-0.19289
54	1	-9.13103	-4.48232	0.580975
55	6	8.410202	-4.49739	0.234449
56	1	8.929867	-4.41743	1.190769
57	1	7.836964	-5.42312	0.192934
58	1	9.130956	-4.48239	-0.58104
59	7	-7.49005	-3.35294	-0.08113
60	7	7.490036	-3.35295	0.081119

### 13. References.

1. C. Xu, and W. W. Webb. *J. Opt. Soc. Am. B* **1996**, *13*, 481.
2. N. S. Makarov, *et. al.* *Optical Materials Express*. **2011**, *4*, 551.
3. Gaussian 09, Revision D.01, M. J. Frisch, G. W. Trucks, H. B. Schlegel, G. E. Scuseria, M. A. Robb, J. R. Cheeseman, G. Scalmani, V. Barone, B. Mennucci, G. A. Petersson, H. Nakatsuji, M. Caricato, X. Li, H. P. Hratchian, A. F. Izmaylov, J. Bloino, G. Zheng, J. L. Sonnenberg, M. Hada, M. Ehara, K. Toyota, R. Fukuda, J. Hasegawa, M. Ishida, T. Nakajima, Y. Honda, O. Kitao, H. Nakai, T. Vreven, J. A. Montgomery, Jr., J. E. Peralta, F. Ogliaro, M. Bearpark, J. J. Heyd, E. Brothers, K. N. Kudin, V. N. Staroverov, T. Keith, R. Kobayashi, J. Normand, K. Raghavachari, A. Rendell, J. C. Burant, S. S. Iyengar, J. Tomasi, M. Cossi, N. Rega, J. M. Millam, M. Klene, J. E. Knox, J. B. Cross, V. Bakken, C. Adamo, J. Jaramillo, R. Gomperts, R. E. Stratmann, O. Yazyev, A. J. Austin, R. Cammi, C. Pomelli, J. W. Ochterski, R. L. Martin, K. Morokuma, V. G. Zakrzewski, G. A. Voth, P. Salvador, J. J. Dannenberg, S. Dapprich, A. D. Daniels, O. Farkas, J. B. Foresman, J. V. Ortiz, J. Cioslowski, and D. J. Fox, Gaussian, Inc., Wallingford CT, 2013.
4. Y. Zhang, J. Wang, P. Ji, X. Yu, H. Liu, X. Liu, N. Zhao, and B. Huang. *Org. Biomol. Chem.* **2010**, *8*, 4582-4588.
5. Chathura S. Abeywickrama, *et.al.* *Chem. Commun.*, **2017**, *53*, 5886-5889.
6. Y. Niko, *et al.* *Sci. Rep.* **2016**, *6*, 18870.
7. Y. Niko, *et al.* *J. Org. Chem. B* **2015**, *80*, 10794-10803.